INFLAMMATION

NLRP3 inflammasome activation triggers gasdermin D–independent inflammation

Chun Wang[1†], Tong Yang[1,2†], Jianqiu Xiao[1†], Canxin Xu[3], Yael Alippe[1], Kai Sun[1,2], Thirumala-Devi Kanneganti[4], Joseph B. Monahan[3], Yousef Abu-Amer[5,6], Judy Lieberman[7], Gabriel Mbalaviele[1]*

NOD-like receptor (NLR), family pyrin domain containing 3 (NLRP3) assembles a protein complex known as the NLRP3 inflammasome upon sensing certain pathogen products or sterile danger signals. Gain-of-function mutations such as the D301N substitution in NLRP3, which cause its constitutive activation (NLRP3^{CA}) also results in inflammasome assembly. This inflammasome processes pro–interleukin-1 β (pro–IL-1β) and pro–IL-18 into bioactive IL-1β and IL-18, respectively, and cleaves gasdermin D (GSDMD). GSDMD amino-terminal fragments form plasma membrane pores that facilitate the secretion of IL-1β and IL-18 and lead to the inflammatory cell death pyroptosis. Accordingly, GSDMD inactivation results in negligible spontaneous inflammation in various experimental models such as in *Nlrp3*$^{CA/+}$ mice lacking GSDMD (*Nlrp3*$^{CA/+}$;*Gsdmd*$^{-/-}$ mice). Here, we found that *Nlrp3*$^{CA/+}$;*Gsdmd*$^{-/-}$ mice, when challenged with LPS or TNF-α, still secreted IL-1β and IL-18, indicating inflammasome activation independent of GSDMD. Accordingly, *Gsdmd*$^{-/-}$ macrophages failed to secrete IL-1β and undergo pyroptosis when briefly exposed to NLRP3 inflammasome activators but released these cytokines when persistently activated. Sustained NLRP3 inflammasome induced caspase-8/-3 and GSDME cleavage and IL-1β maturation in vitro in *Gsdmd*$^{-/-}$ macrophages. Thus, a salvage inflammatory pathway involving caspase-8/-3–GSDME was activated after NLRP3 activation when the canonical NLRP3-GSDMD signaling was blocked. Consistent with genetic data, the active metabolite of FDA-approved disulfiram CuET, which inhibited GSDMD and GSDME cleavage in macrophages, reduced the severe inflammation and tissue damage that occurred in the *Nlrp3*$^{CA/+}$ mice. Thus, NLRP3 inflammasome activation overwhelms the protection afforded by GSDMD deficiency, rewiring signaling cascades through mechanisms that include GSDME to propagate inflammation.

INTRODUCTION

The innate immune receptor nucleotide-binding oligomerization domain–like receptor (NLR), family pyrin domain containing 3 (NLRP3) assembles an intracellular protein complex known as the NLRP3 inflammasome upon sensing plasma membrane perturbations caused by certain microbial products or sterile danger signals (*1*–*3*). This inflammasome leads to cell death and inflammatory responses. The macromolecular structure of the inflammasome is formed by NLRP3, the adaptor protein apoptosis-associated speck-like protein containing a caspase recruitment domain (ASC), and caspase-1, which becomes activated when it is recruited to inflammasomes. Caspase-1, which is activated by all the canonical inflammasomes, cleaves inactive pro–interleukin-1β (pro–IL-1β) and pro–IL-18 into bioactive IL-1β and IL-18, respectively (*2*, *3*); it also cleaves gasdermin D (GSDMD), generating N-terminal fragments that oligomerize within the plasma membrane to form pores through which IL-1β and IL-18 are secreted (*4*–*8*). Excessive pore formation compromises the integrity of the plasma membrane, causing a lytic form of cell death known as pyroptosis. In some situations, cells can survive GSDMD activation but still release inflammatory cytokines in a GSDMD-dependent process, thus have been termed "hyperactivated" (*6*). Pyroptosis is a double-edged sword—it releases inflammatory factors that recruit immune cells to sites of pathogenic infection, which attack and phagocytose pathogens, destroy their replication niches, and boost adaptive immune responses (*9*, *10*). However, excessive or uncontrolled pyroptosis and inflammatory cytokine release can lead to organ damage, circulatory collapse, or even death (*11*–*13*).

GSDMD is also cleaved by caspase-11 (mouse ortholog of human caspase-4 and caspase-5) (*14*), neutrophil elastase and cathepsin G (*15*–*18*), caspase-3 (*19*), and caspase-8 (*20*, *21*). Cleavage by all of these proteases—except caspase-3, which inactivates GSDMD—produces a pore-forming N-terminal fragment. Caspase-3 also cleaves GSDME (also known as DNFA5), producing active N-terminal fragments whose pore-forming activity promotes pyroptosis in response to apoptotic stimuli (*22*–*24*), including chemotherapeutic drugs (*25*, *26*), *Yersinia* infection (*20*), glucocorticoid treatment (*24*), and inflammasome activators in cells lacking GSDMD or caspase-1 (*27*, *28*). GSDME is also a substrate of granzyme B (*23*, *29*). The role of GSDME in cell death may be cell context dependent, because it is seemingly dispensable for pyroptosis in certain cell types or experimental conditions (*19*, *20*, *30*–*33*). The function of GSDME in mediating the release of inflammatory cytokines is less studied. A recent study reported that IL-1α was secreted through GSDME conduits in *caspase-1*– and *caspase-11*–deficient macrophages, but pro–IL-1β was neither processed nor released (*28*). Thus, like GSDMD, cleaved GSDME generates pore-forming fragments that can release cytokines and cause pyroptosis.

Chronic activation of the NLRP3 inflammasome by endogenous host danger-associated molecular patterns and the ensuing excessive

[1]Division of Bone and Mineral Diseases, Washington University School of Medicine, St. Louis, MO 63110, USA. [2]Department of Spine Surgery, Honghui Hospital, Xi'an Jiaotong University, Xi'an, Shaanxi, China. [3]Aclaris Therapeutics Inc., St. Louis, MO 63108, USA. [4]Department of Immunology, St. Jude Children's Research Hospital, Memphis, TN 38105, USA. [5]Department of Orthopaedic Surgery, Washington University School of Medicine, St. Louis, MO, USA. [6]Shriners Hospital for Children, St. Louis, MO 63110, USA. [7]Program in Cellular and Molecular Medicine, Boston Children's Hospital and Department of Pediatrics, Harvard Medical School, Boston, MA 02115 USA.
*Corresponding author. Email: gmbalaviele@wustl.edu
†These authors contributed equally to this work.

production of IL-1β and IL-18 underlie the pathogenesis of several autoimmune and autoinflammatory diseases, including inflammatory bowel disease (*34*–*36*) and rheumatoid arthritis (*37*–*39*), and contribute to the severity of atherosclerosis (*40*, *41*), gout (*42*–*45*), and diabetes (*46*). Gain-of-function mutations in *NLRP3* cause a spectrum of autoinflammatory disorders known as cryopyrin-associated periodic syndromes (CAPS), whose severity is linked to specific *NLRP3* mutations. Neonatal-onset multisystem inflammatory disease (NOMID) is the most severe, and familial cold autoinflammatory syndrome (FCAS) and Muckle-Wells syndrome (MWS) are less severe (*12*, *13*). Clinical manifestations of CAPS include systemic inflammation; skin lesions; central nervous system symptoms including headache, hearing loss, and learning difficulties; and skeletal anomalies (*13*, *47*–*51*). Mice genetically engineered to express NLRP3 variants that harbor mutations found in patients with CAPS ($NLRP3^{CA}$) develop severe systemic inflammation characterized by excessive secretion of IL-1β and IL-18, multiorgan damage, and premature death (*52*, *53*). Although young NOMID mice lacking the IL-1 receptor do not develop inflammation (*54*), a persistent low-grade inflammation is reported in FCAS mice and MWS mice with defective IL-1 and IL-18 signaling (*55*), suggesting that pyroptosis may be the culprit. In support of this view, knocking out *Gsdmd* prevents the pathogenesis of NOMID (*56*), familial Mediterranean fever (FMF) (*57*), and experimental autoimmune encephalitis (*58*). However, how these mutant mice with an underlying dysregulated NLRP3 inflammasome activity withstand superimposed inflammatory challenges has not been studied.

CAPS and several other diseases of dysregulated inflammasome activity, including FMF and macrophage activation syndrome, which are caused by *PYRIN* and *NLRC4* mutations, respectively, are treated with IL-1 blockers (*59*). These therapies have substantially improved the quality of life of affected individuals, but the disease does not always resolve (*60*–*63*). The underlying mechanisms of resistance are not understood, but lingering low-grade inflammation driven by IL-18 and pyroptosis is suspected. To identify drugs that block the integrating nodes of inflammasome signaling, recent studies screened several safe marketed drugs for anti-GSDMD activity. They identified disulfiram, also known as Antabuse, a U.S. Food and Drug Administration (FDA)–approved drug for the treatment of alcohol addiction, and dimethyl fumarate, also known as Tecfidera used to treat multiple sclerosis, as inhibitors of GSDMD and pyroptosis (*64*, *65*). Both drugs also inhibited lipopolysaccharide (LPS)–induced IL-1β and IL-18 secretion in vitro and in vivo (*66*). These observations provide a rationale for evaluating pyroptosis inhibitors in animal inflammasomopathy models.

In this study, we used mice bearing one allele of *Nlrp3* with D301N substitution, which induces constitutive activation of NLRP3 ($NLRP3^{CA}$), and challenged them with inflammatory stimuli [LPS or tumor necrosis factor–α (TNF-α)] to understand better the role of GSDMD in promoting inflammation. We found that NLRP3 inflammasome activation caused IL-1 family cytokine secretion and pyroptosis in $Gsdmd^{-/-}$ macrophages, responses that were associated with caspase-8/-3 and GSDME cleavage. The active metabolite of disulfiram, bis(diethyldithiocarbamate)–copper (CuET), inhibited the cleavage of both GSDMD and GSDME as well as ASC activation, protecting mice from the pathology caused by dysregulated NLRP3 inflammasome. Thus, the inflammatory actions of dysregulated NLRP3 inflammasome involve GSDME in $Gsdmd^{-/-}$ cells and are inhibited by CuET.

RESULTS

Gsdmd-deficient mice expressing hyperactive NLRP3 inflammasome aged normally

D301N substitution in NLRP3 imposes conformational changes and constitutive activation of NLRP3 ($NLRP3^{CA}$); this autosomal dominant mutation causes an inflammatory disease in $Nlrp3^{CA/+}$ mice that resembles human NOMID (*52*, *67*). Most $Nlrp3^{CA/+}$ mice die prematurely about 3 weeks of age because of severe systemic inflammation that damages multiple organs, including the skin, brain, bones, and spleen (*52*, *67*, *68*). $Gsdmd^{-/-}$ and $Nlrp3^{CA/+}$ mice lacking GSDMD ($Nlrp3^{CA/+}$;$Gsdmd^{-/-}$ mice) grow normally and are indistinguishable from their wild-type (WT) counterparts when monitored for up to 66 days, indicating strong GSDMD dependence of inflammation in NOMID mice (*56*). However, mice expressing constitutively activated NLRP3 as a result of L351P substitution that are genetically deficient in *Il-1* and *Il-18* unexpectedly show signs of lingering inflammation (*55*). This finding prompted us to monitor $Nlrp3^{CA/+}$;$Gsdmd^{-/-}$ mice for longer time periods. Mouse survival, white blood cell (WBC) counts, and spleen weight of $Nlrp3^{CA/+}$;$Gsdmd^{-/-}$ and

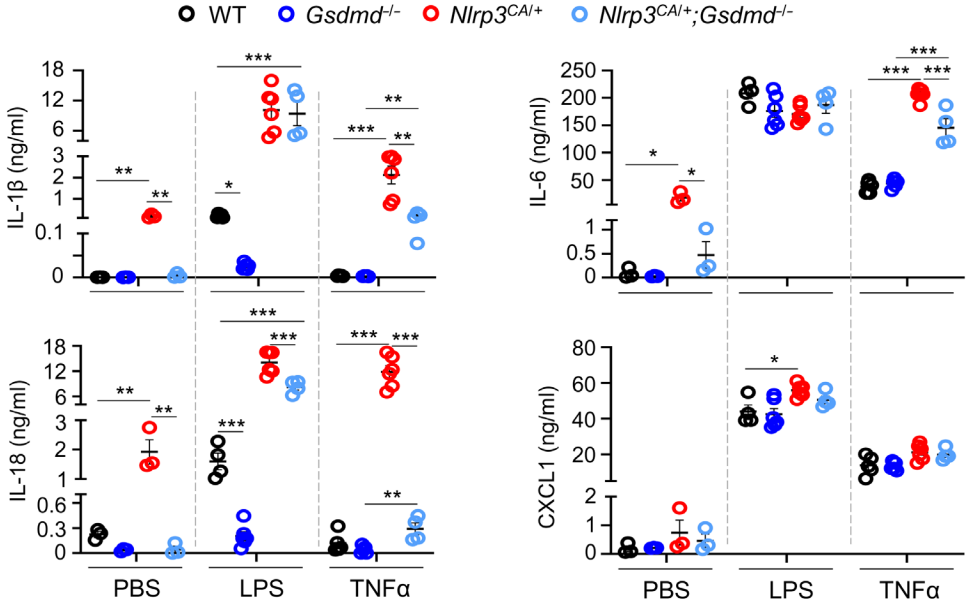

Fig. 1. LPS or TNF-α induced IL-1β and IL-18 secretion in $Nlrp3^{CA/+}$;$Gsdmd^{-/-}$ but not $Gsdmd^{-/-}$ mice. Three-month-old WT, $Gsdmd^{-/-}$, $Nlrp3^{CA/+}$, and $Nlrp3^{CA/+}$;$Gsdmd^{-/-}$ mice were injected with LPS (15 mg/kg) for 6 hours or TNF-α (0.5 mg/kg) for 2 hours. PBS-administrated mice served as controls. $N = 4$ to 6 mice per group. Serum cytokine levels were measured by the V-PLEX Plus Proinflammatory Panel 1 Mouse Kit, except for IL-18, which were assessed by ELISA. Data are means ± SEM. $^*P < 0.05$, $^{**}P < 0.01$, and $^{***}P < 0.001$. One-way ANOVA.

Gsdmd$^{-/-}$ mice remained indistinguishable at 6 and 12 months of age (fig. S1A). Accordingly, the architecture of the spleen and the liver was histologically similar between both genotypes (fig. S1, B and C). Thus, *Nlrp3*$^{CA/+}$;*Gsdmd*$^{-/-}$ mice age normally in homeostatic conditions, consistent with our previous study (*56*).

LPS or TNF-α induced IL-1β and IL-18 secretion in *Nlrp3*$^{CA/+}$;*Gsdmd*$^{-/-}$ but not *Gsdmd*$^{-/-}$ mice

Gsdmd$^{-/-}$ mice, unlike caspase-11$^{-/-}$ mice, are not fully protected from death caused by a lethal dose of LPS (*14*), suggesting that there might be a GSDMD-independent inflammatory pathway. Baseline blood serum IL-1β, IL-18, and IL-6 were low and comparable in WT and *Gsdmd*$^{-/-}$ mice but were constitutively increased in *Nlrp3*$^{CA/+}$ mice and returned to normal in *Nlrp3*$^{CA/+}$;*Gsdmd*$^{-/-}$ mice as expected (Fig. 1). After LPS challenge, serum IL-1β and IL-18 increased in WT mice but not in *Gsdmd*$^{-/-}$ mice. However, in *Nlrp3*$^{CA/+}$ mice, these cytokine levels were about 10-fold higher than in LPS-stimulated WT mice and, unexpectedly, were not substantially reduced in *Nlrp3*$^{CA/+}$;*Gsdmd*$^{-/-}$ mice. LPS stimulated high serum levels of IL-6 and CXCL1 in all the genotypes. TNF-α injection increased serum IL-1β and IL-18 in *Nlrp3*$^{CA/+}$ but not in WT or *Gsdmd*$^{-/-}$ mice, but this increase was significantly reduced but not eliminated in *Nlrp3*$^{CA/+}$;*Gsdmd*$^{-/-}$ mice. TNF-α also elevated serum IL-6 and CXCL1 in all genotypes but induced more IL-6 in *Nlrp3*$^{CA/+}$ mice, which was still above the level in WT mice (Fig. 1). These results indicate that both GSDMD-dependent and GSDMD-independent inflammation is induced in the setting of intense NLRP3 inflammasome activation.

LPS stimulated IL-1β release and GSDME cleavage by *Nlrp3*$^{CA/+}$;*Gsdmd*$^{-/-}$ BMDMs

To examine how GSDMD deficiency affects IL-1β secretion in vitro, we measured its levels after treatment of WT, *Nlrp3*$^{CA/+}$, or *Nlrp3*$^{CA/+}$;*Gsdmd*$^{-/-}$ bone marrow–derived macrophages (BMDMs) primed with LPS and exposed to nigericin, which induces the assembly of the NLRP3 inflammasome (*56*). LPS alone induced IL-1β secretion in *Nlrp3*$^{CA/+}$ cells (Fig. 2A). Nigericin increased the release of IL-1β by LPS-primed cells in the three genotypes, although this response was delayed in double mutant cells, reaching levels comparable to WT and *Nlrp3*$^{CA/+}$ cells by 2 hours. We also assessed cell death by measuring the release of lactate dehydrogenase (LDH) into the cell supernatant. Although LPS and nigericin were required for LDH release from WT BMDMs, endotoxin alone induced these responses in *Nlrp3*$^{CA/+}$ and *Nlrp3*$^{CA/+}$;*Gsdmd*$^{-/-}$ cells, although this

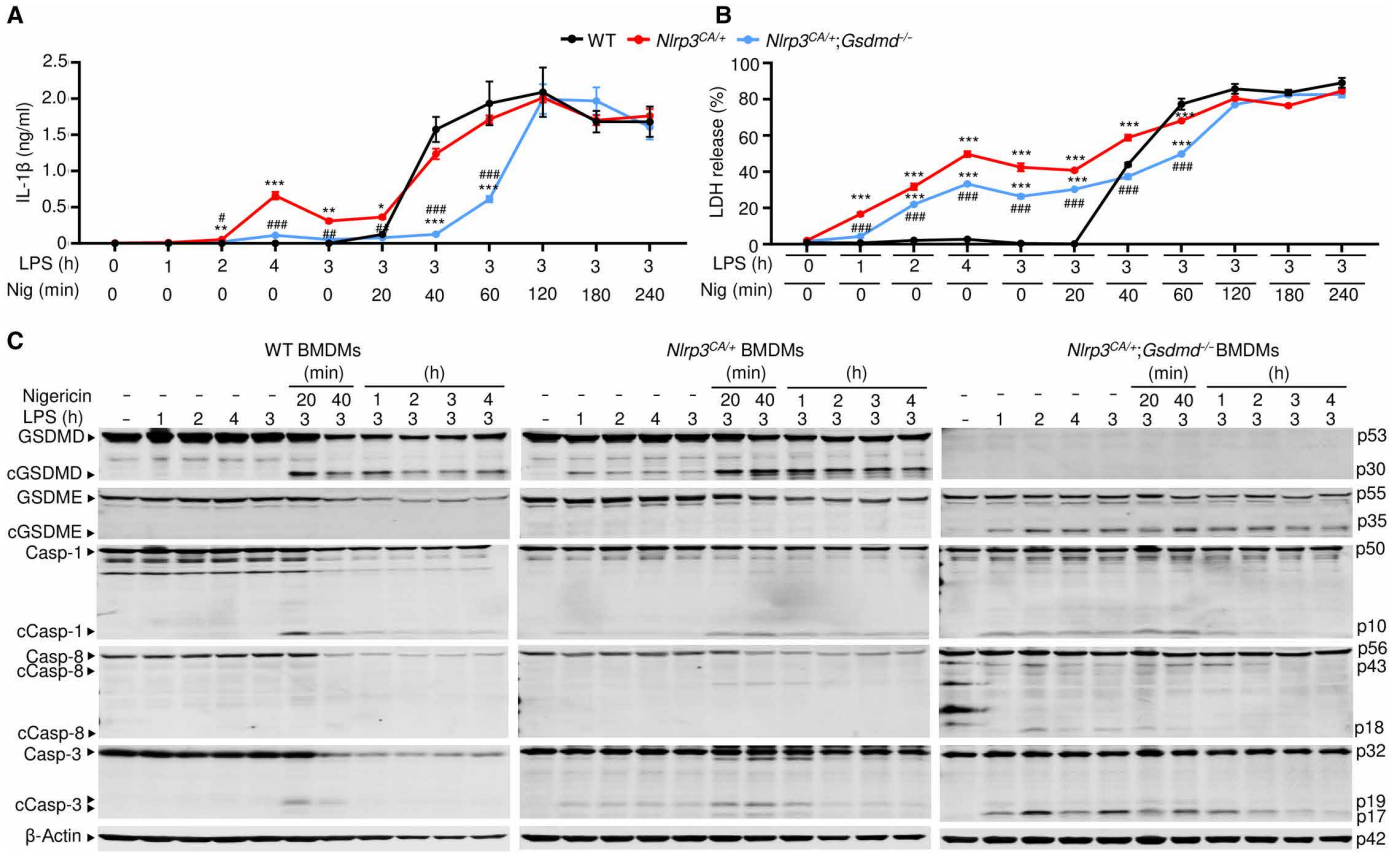

Fig. 2. LPS stimulated IL-1β release and GSDME cleavage by *Nlrp3*$^{CA/+}$;*Gsdmd*$^{-/-}$ BMDMs. BMDMs were expanded in vitro in M-CSF–containing media from bone marrow cells isolated from WT, *Nlrp3*$^{CA/+}$, or *Nlrp3*$^{CA/+}$;*Gsdmd*$^{-/-}$ mice. BMDMs were primed with LPS (100 ng/ml) for 1, 2, 3, or 4 hours and treated with 15 μM nigericin for 20 or 40 min or 1, 2, 3, or 4 hours. IL-1β (**A**) and LDH (**B**) in the conditioned media were measured by ELISA and by a cytotoxicity detection kit, respectively. (**C**) The indicated proteins in the whole-cell lysates were analyzed by immunoblotting. Data are means ± SEM from experimental triplicates and are representative of at least three independent experiments. $^{**}P < 0.01$, $^{***}P < 0.001$, $^{\#\#}P < 0.01$, and $^{\#\#\#}P < 0.001$. ** and ***$Nlrp3^{CA/+}$ or $Nlrp3^{CA/+}$;$Gsdmd^{-/-}$ compared with WT; ## and ###$Nlrp3^{CA/+}$;$Gsdmd^{-/-}$ compared with $Nlrp3^{CA/+}$. One-way ANOVA. cCasp, cleaved caspase; cGSDM, cleaved GSDM; h, hour; min, minute.

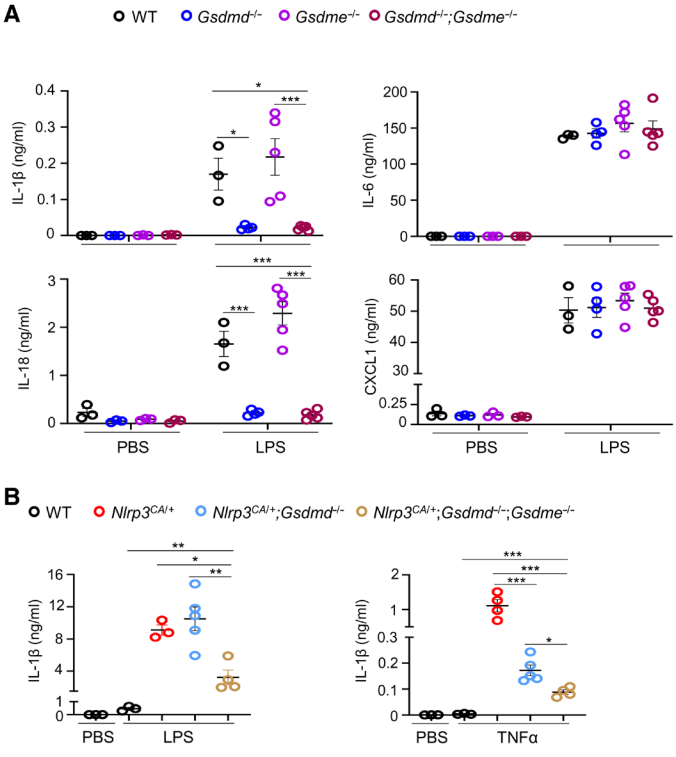

Fig. 3. GSDME was involved in IL-1β and IL-18 secretion induced by LPS or TNF-α in *Nlrp3*$^{CA/+}$;*Gsdmd*$^{-/-}$ mice. Three-month-old WT, *Gsdmd*$^{-/-}$, *Gsdme*$^{-/-}$, *and Gsdmd*$^{-/-}$;*Gsdme*$^{-/-}$ mice (**A**) or WT, *Nlrp3*$^{CA/+}$, *Nlrp3*$^{CA/+}$;*Gsdmd*$^{-/-}$, and *Nlrp3*$^{CA/+}$;*Gsdmd*$^{-/-}$;*Gsdme*$^{-/-}$ mice (**B**) were injected with LPS (15 mg/kg) for 6 hours or TNF-α (0.5 mg/kg) for 2 hours. PBS-administrated mice served as controls. *N* = 3 to 5 mice per group. Serum cytokine levels were measured by the V-PLEX Plus Proinflammatory Panel 1 Mouse Kit, except for IL-18, which were assessed by ELISA. Data are means ± SEM. ***$P < 0.001$. One-way ANOVA.

response was attenuated in double mutant cells and enhanced by nigericin in both genotypes (Fig. 2B). Although GSDMs are the executioners of pyroptosis, mixed lineage kinase domain-like (MLKL) pseudokinase plays a critical role in the cell death necroptosis, the programmed form of necrosis. MLKL perforates the plasma cell membrane and executes necroptosis upon phosphorylation by receptor-interacting serine/threonine kinase 3 (RIPK3) (*69*, *70*). We determined whether MLKL was involved in the responses of *Nlrp3*$^{CA/+}$;*Gsdmd*$^{-/-}$ BMDMs. MLKL was not phosphorylated in *Nlrp3*$^{CA/+}$;*Gsdmd*$^{-/-}$ BMDMs treated with LPS or LPS plus nigericin (fig. S2), suggesting that the delayed death of these cells was necroptosis independent. Thus, IL-1β secretion and pyroptosis are attenuated in *Nlrp3*$^{CA/+}$;*Gsdmd*$^{-/-}$ compared with WT and *Nlrp3*$^{CA/+}$ BMDMs in response to NLRP3 inflammasome activators. However, these responses are undistinguishable among the three cell types where the NLRP3 inflammasome is persistently activated.

To study NLRP3 inflammasome signaling in GSDMD-sufficient or GSDMD-insufficient cells, we treated WT, *Nlrp3*$^{CA/+}$, and *Nlrp3*$^{CA/+}$;*Gsdmd*$^{-/-}$ BMDMs with LPS in the absence or presence of nigericin. Although the combination of LPS and nigericin was required for the formation of ASC specks, a readout of activated inflammasomes (fig. S3) and the cleavage of GSDMD and caspase-1 in WT BMDMs, LPS alone induced these responses in *Nlrp3*$^{CA/+}$ and *Nlrp3*$^{CA/+}$;*Gsdmd*$^{-/-}$ cells (Fig. 2C and fig. S3), consistent with the constitutively activated state of NLRP3 (*52*). However, the combination of LPS and nigericin caused more GSDMD and caspase-1 cleavage than LPS alone in cells with constitutively active NLRP3 (Fig. 2C). Whenever caspase-1 was cleaved in these cells, there was a faint caspase-8/-3 cleavage band. Although full-length GSDME was easily visualized in WT and *Nlrp3*$^{CA/+}$ BMDMs, cleavage of GSDME was not readily detected. However, in *Nlrp3*$^{CA/+}$;*Gsdmd*$^{-/-}$ cells, although basal levels of caspase-8/-3 and GSDME appeared similar to levels in WT or *Nlrp3*$^{CA/+}$ BMDMs, cleaved caspase-8 (p18 fragment) and caspase-3 (p17 fragment), which are fully active, were more prominent, and GSDME cleavage was readily detected (Fig. 2C). Neither GSDME nor caspase-8/-3 cleavage in *Nlrp3*$^{CA/+}$;*Gsdmd*$^{-/-}$ BMDMs required nigericin. Thus, in *Nlrp3*$^{CA/+}$;*Gsdmd*$^{-/-}$ cells, caspase-8/-3 and GSDME are activated by LPS.

GSDME was involved in IL-1β and IL-18 secretion induced by LPS or TNF-α in *Nlrp3*$^{CA/+}$;*Gsdmd*$^{-/-}$ mice

To determine whether GSDMD-independent inflammation in LPS-treated mice might be due to GSDME activation, we first compared baseline and LPS-stimulated blood serum cytokines (IL-1β, IL-18, IL-6, and CXCL1) in *Gsdme*$^{-/-}$ and *Gsdmd*$^{-/-}$;*Gsdme*$^{-/-}$ animals bearing unmutated *Nlrp3*. Baseline cytokine levels were comparable between *Gsdme*$^{-/-}$ and *Gsdmd*$^{-/-}$;*Gsdme*$^{-/-}$ mice and were similar to levels in WT animals (Fig. 3A). After LPS challenge, the IL-1 family cytokines were similarly elevated in *Gsdme*$^{-/-}$ mice as in WT mice but did not increase in *Gsdmd*$^{-/-}$;*Gsdme*$^{-/-}$ animals. LPS induced elevated IL-6 and CXCL1 in all genotypes. Next, we measured IL-1β levels in response to LPS or TNF-α in, *Nlrp3*$^{CA/+}$, *Nlrp3*$^{CA/+}$;*Gsdmd*$^{-/-}$, and *Nlrp3*$^{CA/+}$;*Gsdmd*$^{-/-}$;*Gsdme*$^{-/-}$ mice. *Nlrp3*$^{CA/+}$;*Gsdme*$^{-/-}$ mice were not generated, because LPS-induced responses were not impaired in *Gsdme*$^{-/-}$ animals (Fig. 3A). LPS or TNF-α induced IL-1β production in *Nlrp3*$^{CA/+}$ and *Nlrp3*$^{CA/+}$;*Gsdmd*$^{-/-}$ mice (Fig. 3B). IL-1β levels were decreased in *Nlrp3*$^{CA/+}$;*Gsdmd*$^{-/-}$;*Gsdme*$^{-/-}$ compared with *Nlrp3*$^{CA/+}$;*Gsdmd*$^{-/-}$ mice. These results suggest that GSDME participates in NLRP3 inflammasome signaling in states of GSDMD deficiency.

GSDME was cleaved in BMDMs lacking GSDMD and involved in IL-1β and LDH release

To further examine the impact of GSDMD and GSDME deficiency on LPS plus nigericin induced pyroptosis and IL-1β processing and release in vitro, we pretreated WT, *Gsdmd*$^{-/-}$, *Gsdme*$^{-/-}$, and *Gsdmd*$^{-/-}$;*Gsdme*$^{-/-}$ BMDMs lacking constitutively activated NLRP3 with LPS for 3 hours and then with nigericin for up to 4 hours. Within 20 min of adding nigericin, caspase-1 and caspase-3 were cleaved in all four cell lines (Fig. 4A and fig. S4, A and B). Similar to our findings in Fig. 3A in *Nlrp3*$^{CA/+}$ BMDMs, in cells bearing unmutated *Nlrp3* treated with LPS and nigericin, GSDMD was cleaved in WT and *Gsdme*$^{-/-}$ BMDMs. Consistent with the notion that caspase-8 directly activates caspase-3, the catalytically active caspase-8 p18 and caspase-3 p17 fragments were both more prominent in cells lacking GSDMD. GSDME cleavage was detected only in *Gsdmd*$^{-/-}$ cells. GSDMD and GSDME cleavage was detected at the same time as caspase activation. Because GSDME was not readily cleaved in WT BMDMs, the time-dependent decline of its levels in WT cells was likely secondary to pyroptosis. Thus, GSDME cleavage occurred after NLRP3 inflammasome activation not only in *Nlrp3*$^{CA/+}$;*Gsdmd*$^{-/-}$ BMDMs (Fig. 3A) but also in *Gsdmd*$^{-/-}$ BMDMs.

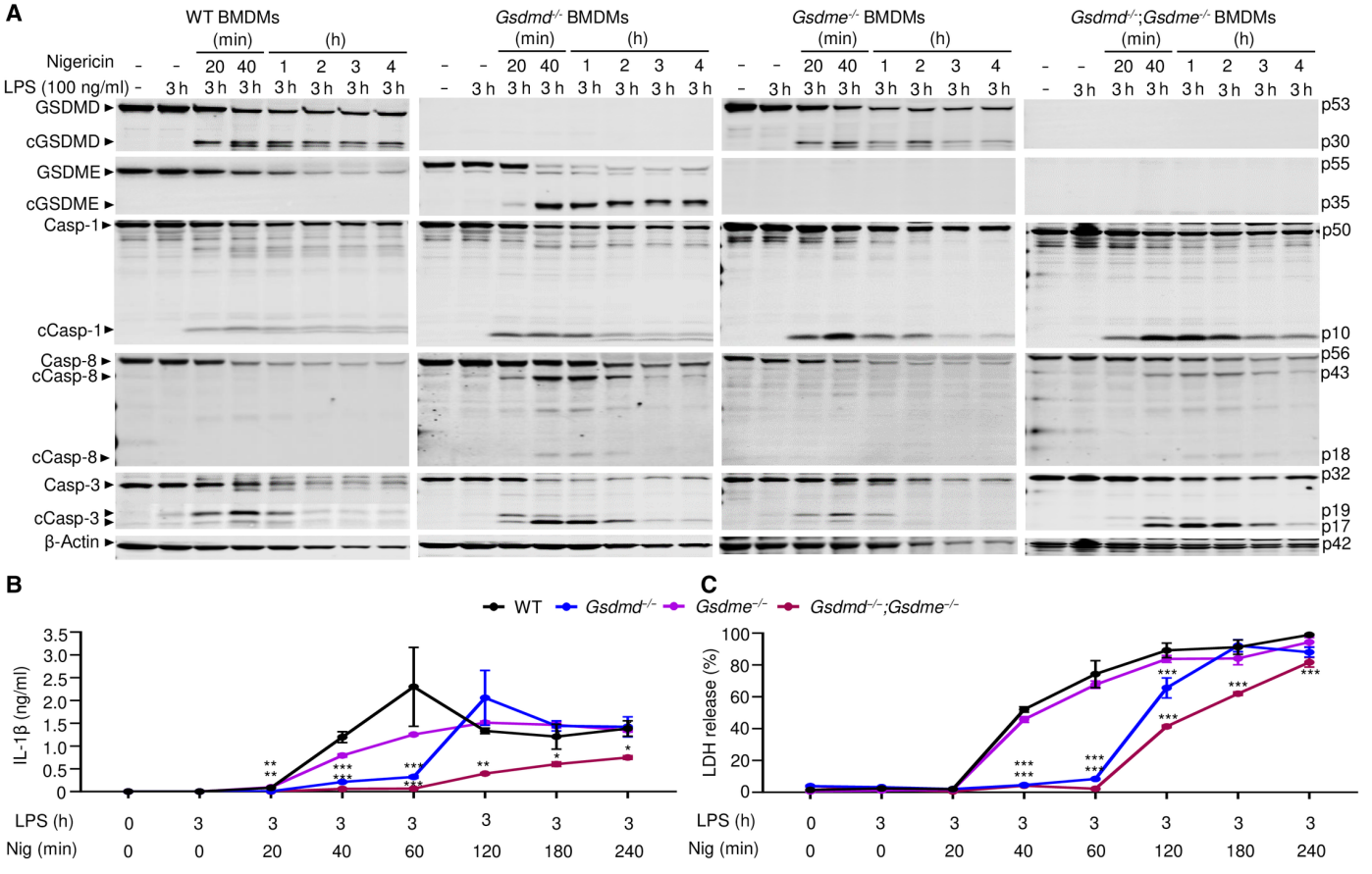

Fig. 4. GSDME was cleaved in *Gsdmd*$^{-/-}$ BMDMs and involved in IL-1β and LDH release. BMDMs from bone marrow isolated from WT, *Gsdmd*$^{-/-}$, *Gsdme*$^{-/-}$, or *Gsdmd*$^{-/-}$;*Gsdme*$^{-/-}$ mice were expanded in vitro in M-CSF–containing media. BMDMs were primed with LPS (100 ng/ml) for 3 hours and treated with 15 μM nigericin for 20 or 40 min or 1, 2, 3, or 4 hours. (**A**) The indicated proteins in the whole-cell lysates were analyzed by immunoblotting. IL-1β (**B**) and LDH (**C**) in the conditioned media were measured by ELISA and by the cytotoxicity detection kit, respectively. Data are means ± SD from experimental triplicates and are representative of at least three independent experiments. *$P < 0.05$, **$P < 0.01$, and ***$P < 0.001$. *, **, and ***compared with WT. One-way ANOVA.

Next, we examined whether caspase-1 was required to activate caspase-3 and GSDME by treating caspase-1–deficient BMDMs with LPS and nigericin. Consistent with previous reports (*71*), LPS and nigericin activated caspase-3 and promoted the generation of the GSDMD p10 fragment in *Casp1*$^{-/-}$ BMDMs, although caspase-3 and GSDMD processing were delayed compared with caspase-1–sufficient cells (fig. S4C). GSDME cleavage was detected in *Casp1*$^{-/-}$ BMDMs at the same time as fully processed caspase-3. Thus, although the maturation of caspase-1 and GSDMD was unperturbed by GSDME deficiency, NLRP3 inflammasome activation forced GSDME processing in cells lacking either caspase-1 or GSDMD.

We examined the extent to which GSDME mediated IL-1β and LDH release in GSDMD-deficient cells. Although LPS-primed *Gsdmd*$^{-/-}$ BMDMs did not release IL-1β or LDH at early time points up to 1 hour after nigericin addition, they were as active as WT cells in secreting IL-1β and releasing LDH at later time points (Fig. 4, B and C) and in dose-dependent manner (fig. S4D). Loss of GSDME did not affect IL-1β and pyroptosis, but these readouts were significantly impaired, but not abrogated, in *Gsdmd*$^{-/-}$;*Gsdme*$^{-/-}$ BMDMs (Fig. 4, B and C). Likewise, LDH release was delayed, and IL-1β levels were nearly undetectable in *caspase-1*$^{-/-}$ BMDMs (fig. S4E), suggesting that cleaved and secreted IL-1β but not intracellular pro–IL-1β was detected in the supernatants of *Nlrp3*$^{CA/+}$;*Gsdmd*$^{-/-}$ (Fig. 3B) or *Gsdmd*$^{-/-}$ (Fig. 4B) BMDM cultures. GSDME cleavage and IL-1β secretion in *Gsdmd*$^{-/-}$ and *Nlrp3*$^{CA/+}$;*Gsdmd*$^{-/-}$ BMDMs induced by LPS and nigericin were inhibited by the pan caspase inhibitor, zVAD (fig. S5, A and B), results that were consistent with the reported cleavage of GSDME by caspase-3 (*22*–*24*). zVAD failed to consistently inhibit LDH release (fig. S5C), and caspase-11 was not activated in these experimental conditions where LPS was added extracellularly (fig. S6A). As a result, GSDME processing (fig. S6A), IL-1β secretion, and LDH release (fig. S6B) were comparable between WT and *caspase-11*$^{-/-}$ BMDMs.

Last, we studied the effects of LPS on WT, *Nlrp3*$^{CA/+}$, *Nlrp3*$^{CA/+}$;*Gsdmd*$^{-/-}$, and *Nlrp3*$^{CA/+}$;*Gsdmd*$^{-/-}$;*Gsdme*$^{-/-}$ BMDMs. LPS alone did not stimulate IL-1β secretion (Fig. 5A) and LDH release (Fig. 5B) in WT cells as expected. LPS induced IL-1β secretion and LDH release in *Nlrp3*$^{CA/+}$ BMDMs; although, the inhibition of this response was transient in *Nlrp3*$^{CA/}$;*Gsdmd*$^{-/-}$ BMDMs (up to 9 hours), it was sustained in *Nlrp3*$^{CA/+}$;*Gsdmd*$^{-/-}$;*Gsdme*$^{-/-}$ BMDMs up to 24 hours (Fig. 5, A and B). Thus, the release of IL-1β and LDH was persistently inhibited, although not completely eradicated, in *Gsdmd*$^{-/-}$;*Gsdme*$^{-/-}$ BMDMs subjected to sustained NLRP3 inflammasome activation.

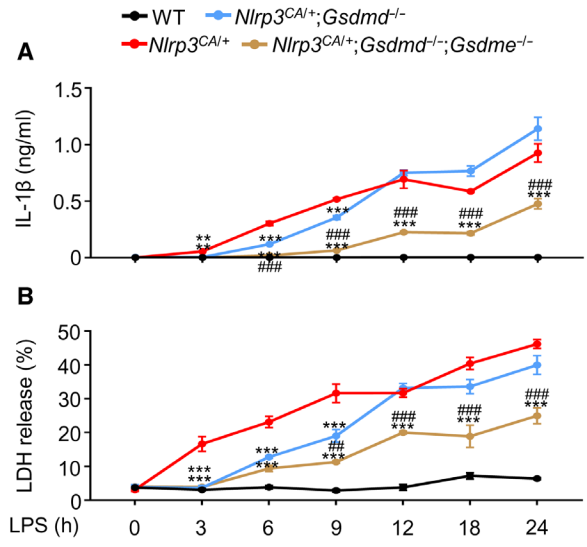

Fig. 5. GSDME was involved in IL-1β and LDH release by *Nlrp3*$^{CA/+}$;*Gsdmd*$^{-/-}$ BMDMs. BMDMs were expanded in vitro in M-CSF–containing media from bone marrow cells isolated from WT, *Nlrp3*$^{CA/+}$, *Nlrp3*$^{CA/+}$;*Gsdmd*$^{-/-}$, and *Nlrp3*$^{CA/+}$;*Gsdmd*$^{-/-}$;*Gsdme*$^{-/-}$ mice. BMDMs were treated with LPS (100 ng/ml) for 3, 6, 9, 12, 18, or 24 hours. IL-1β (**A**) and LDH (**B**) in the conditioned media were measured by ELISA and by a cytotoxicity detection kit, respectively. Data are means ± SEM from experimental triplicates and are representative of at least three independent experiments. $^{**}P < 0.01$; $^{***}P < 0.001$; $^{\#\#}P < 0.01$; $^{\#\#\#}P < 0.001$. ****Nlrp3*$^{CA/+}$;*Gsdmd*$^{-/-}$ or *Nlrp3*$^{CA/+}$;*Gsdmd*$^{-/-}$;*Gsdme*$^{-/-}$ compared with *Nlrp3*$^{CA/+}$; $^{\#\#\#}$*Nlrp3*$^{CA/+}$;*Gsdmd*$^{-/-}$;*Gsdme*$^{-/-}$ compared with *Nlrp3*$^{CA/+}$;*Gsdmd*$^{-/-}$. One-way ANOVA.

CuET inhibited GSDMD, GSDME, and IL-1β maturation and LDH release

Disulfiram and its active metabolite, CuET, antagonize GSDMD pore-forming activity but have not been reported to inhibit GSDME pore formation (*64*). To investigate whether these compounds might inhibit GSDMD-independent pyroptosis, WT, *Gsdmd*$^{-/-}$, *Gsdme*$^{-/-}$, and *Gsdmd*$^{-/-}$;*Gsdme*$^{-/-}$ BMDMs were treated with LPS for 3 hours and then with CuET or vehicle for 1 hour followed by an additional 3 hours of incubation with nigericin. In the absence of CuET, GSDMD was cleaved in WT and *Gsdme*$^{-/-}$ BMDMs (Fig. 6A) and caspase-1–deficient BMDMs (fig. S7A), consistent with the results shown in Fig. 4. Although GSDME was cleaved only in *Gsdmd*$^{-/-}$ cells, caspase-1 and caspase-3 were cleaved in all cell lines. However, although the full-length caspase protein bands sharply decreased, the signals of their cleaved fragments were faint (Fig. 6A), presumably because they might have been released to the extracellular milieu during pyroptosis (*72*–*74*), which was maximal in cells treated with nigericin for 2 hours. GSDMD, GSDME, and caspase-1 cleavage were consistently inhibited by CuET in a dose-dependent manner (Fig. 6A and fig. S7A). The band for cleaved caspase-3 was more prominent in CuET-treated than untreated WT, *Gsdmd*$^{-/-}$, and *Gsdme*$^{-/-}$ BMDMs. CuET inhibited the release of IL-1β and LDH in all cell genotypes (Fig. 6, B and C, and fig. S7B) but was less efficacious in *Gsdmd*$^{-/-}$;*Gsdme*$^{-/-}$ BMDMs in which cytokine release and pyroptosis were attenuated (Fig. 6, B and C). Disulfiram and CuET both inhibited IL-1β and LDH release in WT BMDMs with comparable dose-response curves (fig. S7, C to F). Thus, CuET inhibits the maturation of both GSDMD and GSDME, inhibiting both GSDMD-dependent and GSDMD-independent pyroptosis and IL-1β release.

CuET inhibited NLRP3 inflammasome–dependent, but not NLRP3 inflammasome–independent, responses

The ability of CuET to inhibit the cleavage of GSDMD and GSDME downstream of caspase-1 and caspase-3, respectively, raises concerns that this compound may act as a pan caspase inhibitor. To determine whether CuET inhibits inflammasome-independent GSDME maturation, BMDMs were treated with raptinal or TNF-α and 5Z-7-oxozeaenol (5Z-7; a transforming growth factor–β–activated kinase-1 inhibitor) in the presence or absence of CuET; both treatments are known to activate caspase-3– and GSDME-dependent pyroptosis independently of any inflammasome (*23*, *75*). CuET did not inhibit the cleavage of GSDMD (to p10 GSDMD), GSDME, or caspase-3 induced by raptinal or TNF-α and 5Z-7 (Fig. 7, A and B, and fig. S8A) and if anything appeared to enhance their cleavage in response to these stimuli (Fig. 7B). To determine why CuET inhibited the cleavage of these proteins in response to NLRP3 inflammasome activation but not apoptotic stimuli, we analyzed its effects on nuclear factor κB (NF-κB) and mitogen-activated protein kinase (MAPK) activation. CuET had no effect on LPS-stimulated phosphorylation of inhibitor of nuclear factor κBα (IκBα), NF-κB/p65, and p38 MAPK (fig. S8B). We also analyzed CuET effects on LPS plus nigericin-induced inflammasome activation by measuring the formation of ASC specks, a key step in inflammasome assembly and activation using WT BMDMs expressing fluorescent *Asc-citrine*. To minimize potential effects of CuET on inflammasome priming signals, we added the drug to LPS-primed cells and immediately followed by adding nigericin. The formation of ASC specks was significantly inhibited by CuET (Fig. 7C). These results suggest that CuET inhibits NLRP3 inflammasome activation, but not GSDME, caspase-3, or LPS-induced NF-κB or MAPK activation.

CuET prevented inflammasomopathy in *Nlrp3*$^{CA/+}$ mice

On the basis of its in vitro potency in inhibiting the release of cytokines and pyroptosis, CuET should improve the disease outcomes of *Nlrp3*$^{CA/+}$ mice. To test this idea, CuET was intraperitoneally injected to 10-day-old pups, once every 2 days (*76*). CuET significantly improved the survival rate of *Nlrp3*$^{CA/+}$ mice (fig. S9A) and reduced splenomegaly in these mice (fig. S9B). Despite improved survival, treated *Nlrp3*$^{CA/+}$ mice still showed early mortality, likely due to the severe inflammation already activated before treatment was initiated. To control the onset of this possible inflammation, we leveraged the *Nlrp3*$^{+/fl(D301N)}$;*Cre-ER* model for postnatal inducible activation of the NLRP3^{CA} (iNLRP3^{CA}) inflammasome in adult mice to test the efficacy of prophylactically administrated CuET. Three-month-old mice were injected with tamoxifen three times per week for 2 weeks. Vehicle or CuET was injected 2 days before starting tamoxifen and continued three times per week for 6 weeks. *iNlrp3*$^{CA/+}$ mice all survived but developed cachexia, splenomegaly, leukocytosis, and neutrophilia, which were significantly attenuated by CuET (Fig. 8A). CuET prevented inflammation in the liver and the disorganization of splenic architecture in *iNlrp3*$^{CA/+}$ mice as assessed by hematoxylin and eosin (H&E) staining and had no apparent effect on these tissues in WT controls (Fig. 8B and fig. S9C). Although the effects of CuET were not analyzed in *Nlrp3*$^{CA/+}$;*Gsdmd*$^{-/-}$ mice because of the limited number of animals for in vivo studies, we determined its actions on these cells in vitro. We found that CuET inhibited

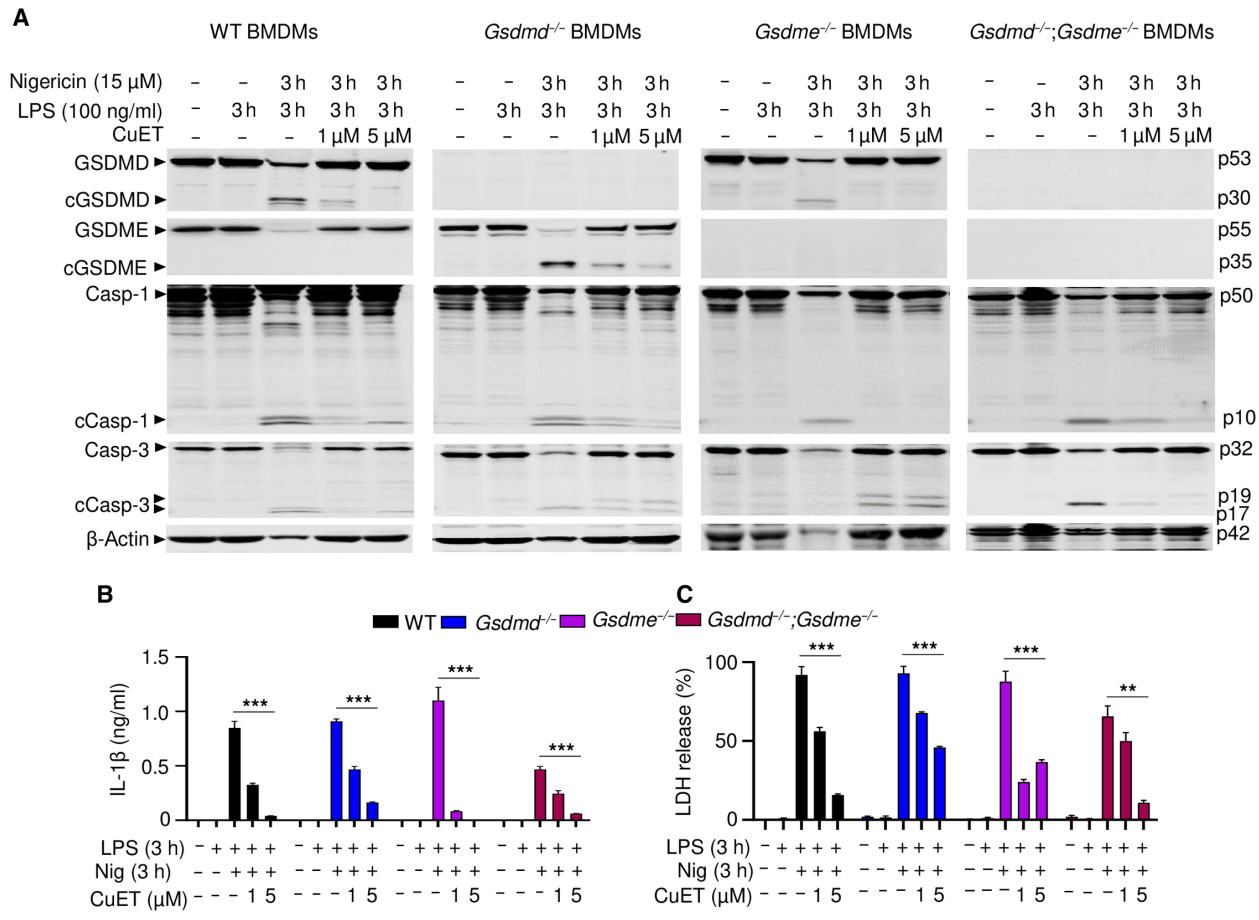

Fig. 6. CuET inhibited GSDMD, GSDME, and IL-1β maturation and LDH release. BMDMs were expanded in vitro in M-CSF–containing media from bone marrow cells isolated from WT, *Gsdmd*$^{-/-}$, *Gsdme*$^{-/-}$, or *Gsdmd*$^{-/-}$;*Gsdme*$^{-/-}$ mice. BMDMs were primed with LPS (100 ng/ml) for 3 hours and treated with vehicle or CuET for 1 hour before adding 15 μM nigericin for 3 hours. (**A**) The indicated proteins in the whole-cell lysates were analyzed by immunoblotting. IL-1β (**B**) and LDH (**C**) in the conditioned media were measured by ELISA and by the cytotoxicity detection kit, respectively. Data are means ± SD from experimental triplicates and are representative of at least three independent experiments. $^{**}P < 0.01$ and $^{***}P < 0.001$. Two-way ANOVA.

GSDME cleavage, IL-1β secretion, and LDH release in WT and *Nlrp3*$^{CA/+}$;*Gsdmd*$^{-/-}$ BMDMs (fig. S10). Thus, our findings show that CuET-treated *Nlrp3*$^{CA/+}$ mice phenocopy *Nlrp3*$^{CA/+}$;*Gsdmd*$^{-/-}$;*Gsdme*$^{-/-}$mice, consistent with the ability of this drug to inhibit GSDMD and GSDME cleavage (fig. S11).

DISCUSSION

Nlrp3$^{CA/+}$ (NOMID) mice die perinatally because of severe systemic multiorgan complications driven by excessive blood levels of IL-1β and IL-18 (*52*, *77*). *Nlrp3*$^{CA/+}$ mice lacking GSDMD (*Nlrp3*$^{CA/+}$;*Gsdmd*$^{-/-}$ mice) grew and aged normally and are fertile. Consistent with these observations, ablation of GSDMD reduces inflammation and improves disease outcomes in mouse models of NOMID, sepsis, FMF, and experimental autoimmune encephalitis (*14*, *56*, *57*, *58*). However, when stressed by exposure to LPS, *Nlrp3*$^{CA/+}$;*Gsdmd*$^{-/-}$ mice unexpectedly secreted high amounts of IL-1β and IL-18. The combination of these inflammatory stimuli with constitutively active NLRP3 overwhelmed the protection provided by GSDMD or caspase-1 deficiency to various extents, rewiring signaling cascades through caspase-3 and GSDME likely to cause pyroptosis (*22*, *25*). These observations suggest that therapeutic inhibition of GSDMD may not be sufficient to prevent complications such as those associated with infections, which have the potential to activate not only GSDMD but also GSDME. This scenario can be tested preclinically by assessing the consequences of infections or injuries in NOMID or FMF mice lacking GSDMD, which can be viewed as animals with an underlying inflammatory condition. Thus, although apparently normal in homeostatic conditions, *Nlrp3*$^{CA/+}$;*Gsdmd*$^{-/-}$ mice are vulnerable to stressful insults.

Both *Nlrp3*$^{CA/+}$;*Gsdmd*$^{-/-}$ BMDMs and *Gsdmd*$^{-/-}$ BMDMs produced IL-1β and underwent pyroptosis in response to LPS, although these responses were delayed in both cell lines compared with WT cells, occurring only upon sustained exposure to NLRP3 inflammasome activators. The responsiveness of *Gsdmd*$^{-/-}$ cells to LPS in vitro suggested that exposure of GSDMD-deficient mice to endotoxin for a long period may lead to significant IL-1β and IL-18 secretion. Consistent with this, a small proportion of *Gsdmd*$^{-/-}$ mice die upon LPS challenge (*14*, *65*). Pyroptosis and cytokine release by GSDMD- or caspase-1–deficient cells positively correlated with caspase-3 and GSDME activation and were significantly suppressed in *Nlrp3*$^{CA/+}$;*Gsdmd*$^{-/-}$;*Gsdme*$^{-/-}$ cells and *Gsdmd*$^{-/-}$;*Gsdme*$^{-/-}$ cells,

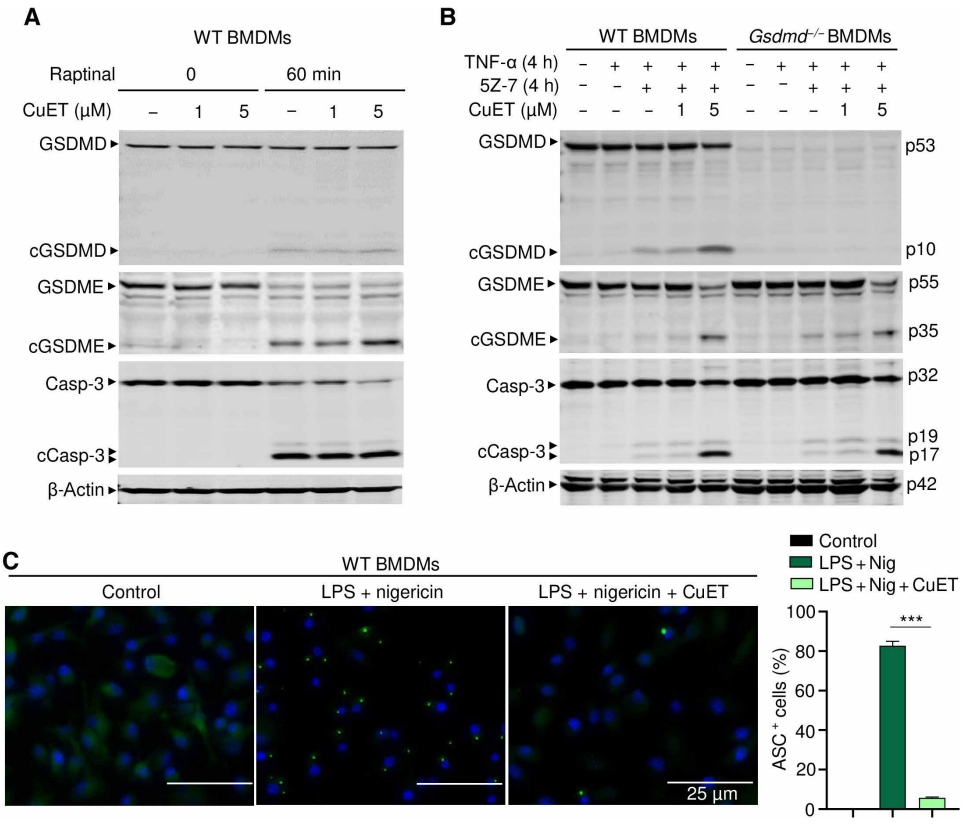

Fig. 7. CuET inhibited NLRP3 inflammasome–dependent but not NLRP3 inflammasome–independent responses. BMDMs were expanded in vitro M-CSF–containing media from bone marrow cells isolated from WT or *Gsdmd*$^{-/-}$ mice. (**A**) WT BMDMs were pretreated with vehicle or CuET for 1 hour and were stimulated with vehicle or 10 μM raptinal for 1 hour. (**B**) WT and *Gsdmd*$^{-/-}$ BMDMs were pretreated with vehicle or CuET for 1 hour and were stimulated with TNF-α (100 ng/ml) and 1 μM 5Z-7 (TAK1 inhibitor) for 4 hours. The indicated proteins in the whole-cell lysates were analyzed by immunoblotting (A and B). (**C**) WT BMDMs from *Asc-citrine* mice were primed with LPS (100 ng/ml) for 3 hours and treated with vehicle or 1 μM CuET for 15 min and then with15 μM nigericin for additional 30 min. ASC specks were visualized under fluorescence microscopy and quantified using ImageJ. Data are means ± SEM from experimental triplicates and are representative of at least three independent experiments. ***$P < 0.001$. One-way ANOVA.

suggesting that caspase-3 activation of GSDME was largely responsible for inflammatory death when NLRP3 was activated, but the canonical caspase-1–GSDMD pathway was not available. Consistent with our findings on GSDM complementation, a recent study reported that the TLR1/TLR2 agonist Pam3CSK4 promotes the release of IL-1α by caspase-1–deficient macrophages through GSDME conduits (*28*). In our study, caspase-3 activation was enhanced by GSDMD or caspase-1 genetic deficiency. We did not explore the mechanism responsible for increased caspase-8 and caspase-3 activation in these settings, but one possibility was that caspase-8 was efficiently recruited to the NLRP3 complex when caspase-1 or GSDMD was absent and very potent at processing caspase-3, which, in turn, activated GSDME. Note that there was some residual IL-1β release and pyroptosis in chronically activated *Nlrp3*$^{CA/+}$;*Gsdmd*$^{-/-}$;*Gsdme*$^{-/-}$ cells and *Gsdmd*$^{-/-}$;*Gsdme*$^{-/-}$ BMDMs, suggesting that another GSDMD- and GSDME-independent inflammation pathway may be activated downstream of NLRP3, potentially involving another caspase and/or another gasdermin. From our study, it remains uncertain whether cytokines are secreted through GSDME pores in the setting of caspase-1 or GSDMD deficiency or are released when the cell membrane is grossly disrupted and LDH is released, as was recently reported (*78*, *79*). Together, these results suggest that macrophages have more than one salvage mechanism to ensure that signals transmitted by inflammasome activators result in inflammation. However, outcomes such as temperature changes and immune cell recruitment to tissues in LPS-treated *Nlrp3*$^{CA/+}$;*Gsdmd*$^{-/-}$;*Gsdme*$^{-/-}$ mice were not assessed in this study but are themes of interest for future investigations.

Drug discovery and repurposing efforts have identified the FDA-approved drugs dimethyl fumarate and disulfiram as GSDMD inhibitors (*64*, *65*). Covalent modification of Cys^{191} in human and Cys^{192} in mouse is the proposed main mechanism through which disulfiram inhibits GSDMD pore-forming activity, although dimethyl fumarate likely works through another mechanism (*65*). Here, we report that the disulfiram metabolite CuET exhibited remarkable efficacy in the *Nlrp3*^{CA} inflammasomopathy model, because it prevented systemic inflammation and the damage to the liver and spleen. Mechanistically, we found that CuET suppressed cytokine secretion and pyroptosis caused by both GSDMD and GSDME. However, CuET inhibited GSDME cleavage and pyroptosis in cells stimulated with NLRP3 inflammasome activators but not apoptotic stimuli. These results ruled out GSDME as the major direct target of CuET inhibitory actions, a view that was consistent with the compound's ability to inhibit the formation of ASC specks. Although, as far as we are aware, direct inhibition of GSDME pore formation by disulfiram has never been measured, Cys$^{191/192}$ is not conserved in mouse GSDME, and therefore, disulfiram is not predicted to be a potent regulator of GSDME. However, as a cysteine-reactive drug, disulfiram has the potential to inactivate other enzymes, including the caspase cysteine proteases and other proteins with reactive cysteines that are modulated by cellular redox status, which include the NLRP3 inflammasome (*80*). When a potent drug target such as GSDMD is not present, disulfiram may switch to inhibit other less reactive substrates, a scenario that may explain the inhibitory effects of CuET in cell lacking GSDMD and GSDME. However, we currently have limited knowledge on the selectivity profile of CuET; thus, future studies will need to investigate how it inhibits ASC polymerization and whether it antagonizes other early steps of inflammasome signaling.

This study revealed that ablation of GSDMD in *Nlrp3*$^{CA/+}$ mice did not prevent these animals from producing excessive levels of IL-1β and IL-18 in response to inflammatory challenges. The disease severity in *Nlrp3*$^{CA/+}$ mice was remarkably reduced by CuET, a drug

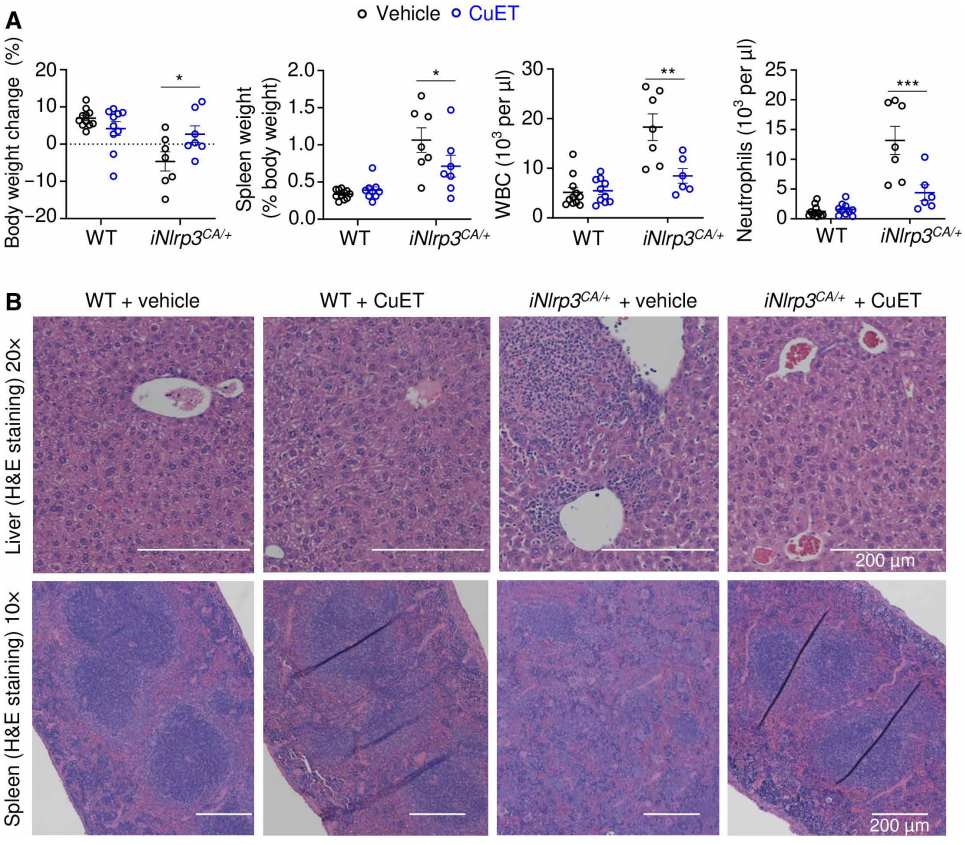

Fig. 8. CuET prevented inflammasomopathy in the inducible *Nlrp3*$^{CA/+}$ (*iNlrp3*$^{CA/+}$) model. Three-month-old mice were injected with tamoxifen once every other day, three times a week for 2 weeks. Injections with vehicle or body weight CuET (1 mg/kg) started 2 days before the tamoxifen regimen and were carried out once every other day, three times a week for 6 weeks. All injections were given intraperitoneally. $N = 6$ to 11 mice per group. (**A**) Body weight change, spleen weight, WBC, and neutrophils. Data are means ± SEM. Two-way ANOVA. *$P < 0.05$, **$P < 0.01$, and ***$P < 0.001$. (**B**) Representative H&E staining of the liver and spleen sections. *iNlrp3*$^{CA/+}$, inducible NLRP3$^{CA/+}$.

that interferes directly or indirectly with both GSDMD-dependent and GSDMD-independent inflammation. Our findings suggest that disulfiram might be worth testing in patients with CAPS for whom existing therapies that inhibit IL-1 or other inflammatory cytokines do not adequately suppress disease symptoms.

MATERIALS AND METHODS

Study design

The objective of this study was to determine the responses of the seemingly normal *Gsdmd*$^{-/-}$ mice expressing constitutive active NLRP3—yet viewed as animals with an underlying inflammatory condition—to inflammatory stimuli (e.g., LPS and TNF-α). To achieve this goal, we used various strategies, including genetic and pharmacological manipulation, biochemical, histology, and immunostaning approaches.

Animals

Casp1$^{-/-}$ mice were provided by T.-D.K. (St. Jude Children's Research Hospital). *Cre-ER* [B6.Cg-Tg(CAG-cre/Esr1*)5Amc/J] mice and *lysozyme M-Cre* mice were purchased from the Jackson Laboratory (Sacramento, CA). *Nlrp3*$^{fl(D301N)/+}$ mice were provided by H. Hoffman (University of California, San Diego) and have been previously described (*52*, *54*, *81*). *Nlrp3*$^{CA/+}$ mice with constitutive activation of NLRP3 in myeloid cells driven by *lysozyme M-Cre* have been previously described (*54*). *Cre-ER* mice and *Nlrp3*$^{fl(D301N)/+}$ mice were crossed to generate *Nlrp3*$^{fl(D301N)/+}$;*Cre-ER* mice and *Cre-ER* mice. Injection of tamoxifen (intraperitoneally, 75 mg/kg body weight; Sigma-Aldrich) to *Nlrp3*$^{fl(D301N)/+}$;*Cre-ER* mice and *Cre-ER* mice to yield inducible *Nlrp3*$^{CA/+}$ (*iNlrp3*$^{CA/+}$) mice and control mice, respectively, has been previously described (*81*). *Gsdmd*$^{-/-}$ mice were provided by V. M. Dixit (Genentech, South San Francisco, CA). *Asc-citrine* and *Gsdme*$^{-/-}$ mice were purchased from the Jackson Laboratory (Sacramento, CA). All mice were on the C57BL6J background, and mouse genotyping was performed by polymerase chain reaction. All procedures were approved by the Institutional Animal Care and Use Committee of Washington University School of Medicine in St. Louis.

Administration of drugs, LPS, and TNF-α

Mice were intraperitoneally injected with CuET (1 mg/kg; TCI America, OR) formulated in sesame oil (0.2 mg/ml) or vehicle, once every other day, three times per week. Ten-day-old *Nlrp3*$^{CA/+}$mice were treated with vehicle or CuET for 9 weeks; 12-week-old *iNlrp3*$^{CA/+}$ and control mice were treated with vehicle or CuET three times per week for 6 weeks. For LPS challenge experiments, WT, *Gsdmd*$^{-/-}$, *Gsdme*$^{-/-}$, *Gsdmd*$^{-/-}$;*Gsdme*$^{-/-}$, *Nlrp3*$^{CA/+}$, *Nlrp3*$^{CA/+}$;*Gsdmd*$^{-/-}$, and *Nlrp3*$^{CA/+}$;*Gsdmd*$^{-/-}$;*Gsdme*$^{-/-}$ mice were intraperitoneally injected with LPS (15 mg/kg) (*Escherichia coli* O111:B4; Sigma-Aldrich, MO). Mice were intraperitoneally injected with TNF-α (0.5 mg/kg; BioLegend, CA).

Serum cytokine assay

Blood was collected by cardiac puncture 6 or 2 hours after LPS or TNF-α challenge and was allowed to clot at room temperature. Serum obtained after centrifugation at 2000*g* for 10 min was used for determinations of cytokine and chemokine levels by the V-PLEX Plus Proinflammatory Panel 1 Mouse Kit (Meso Scale Diagnostics, MD), except IL-18, which was analyzed by an enzyme-linked immunosorbent assay (ELISA) kit (Sigma-Aldrich, MO).

Cell cultures

BMDMs were obtained by culturing mouse bone marrow cells in culture media containing a 1:10 dilution of supernatant from the fibroblastic cell line CMG 14-12 as a source of macrophage colony-stimulating factor (M-CSF) (*82*), a mitogenic factor for BMDMs, for 4 to 5 days in a 15-cm dish as previously described (*81*). Briefly,

nonadherent cells were removed by vigorous washes with phosphate-buffered saline (PBS), and adherent BMDMs were detached with trypsin-EDTA and cultured in culture media containing a 1:10 dilution of CMG for various experiments.

For all in vitro pharmacology experiments except otherwise specified, cells were pretreated with vehicle [0.1% dimethyl sulfoxide (DMSO), final concentration] or inhibitors (in 0.1% DMSO, final concentration) for 1 hour before stimulation with the indicated ligand or ligands. Protein expression was analyzed by ELISA or Western blot as described below. To activate the NLRP3 inflammasome, BMDMs were plated at 10^4 cells per well on a 96-well plate or 10^6 cells per well on a six-well plate overnight. Cells were primed with LPS and then with 15 μM nigericin (AdipoGen) as indicated, and conditioned media were collected for the analysis of IL-1β and LDH.

Histology

Tissue samples were processed as described previously (*81*). Briefly, the liver and spleen were fixed in 10% formalin overnight. Fixed tissues were embedded in paraffin, sectioned at 5-μm thicknesses, and mounted on glass slides. The sections were stained with H&E as described previously (*81*). Photographs were taken using ZEISS microscopy (Carl Zeiss Industrial Metrology, MN).

Peripheral blood analyses

Mouse blood was collected by cardiac puncture in the EDTA-containing tubes. Complete blood counts were performed by the Washington University School of Medicine as previously described (*54*).

Western blot analysis

Cell extracts were prepared by lysing cells with radioimmunoprecipitation assay (RIPA) buffer (50 mM tris, 150 mM NaCl, 1 mM EDTA, 0.5% NaDOAc, 0.1% SDS, and 1.0% NP-40) plus phosphatase and protease inhibitors (2 mM NaVO4, 10 mM NaF, and 1 mM phenylmethylsulfonyl fluoride) and complete protease inhibitor cocktail (Roche, CA). For tissue extracts, liver tissues were homogenized and lysed with RIPA buffer containing phosphatase and protease inhibitors. Protein concentrations were determined by the Bio-Rad Laboratories method, and equal amounts of proteins were subjected to SDS–polyacrylamide gel electrophoresis gels (12%) as previously described (*56*). Proteins were transferred onto nitrocellulose membranes and incubated with antibodies against GSDMD (1:1000; Abcam, MA), GSDME (1:1000; Abcam, MA), caspase-1 (1:1000; Abcam, MA), caspase-3 (1:1000; Cell Signaling Technology, MA), p38 MAPK (1:1000; Cell Signaling Technology, MA), β-actin (1:2000; Santa Cruz Biotechnology, TX), p65/p-p65 (1:1000; Cell Signaling Technology, MA), IκBα/p-IκBα (1:1000; Cell Signaling Technology, MA), or pMLKL (1:1000; Cell Signaling Technology, MA) overnight at 4°C followed by incubation for 1 hour with secondary goat anti-mouse IRDye 800 (Thermo Fisher Scientific, MA) or goat anti-rabbit Alexa Fluor 680 (Thermo Fisher Scientific, MA), respectively. The results were visualized using the Odyssey Infrared Imaging System (LI-COR Biosciences, NE).

LDH assay and IL-1β ELISA

Cell death was assessed by the release of LDH in conditioned medium using the LDH Cytotoxicity Detection Kit (Takara, CA). IL-1β levels in conditioned media were measured by an ELISA kit (eBioscience, NY).

ASC specks assay

Asc-citrine, WT, and *Nlrp3*$^{CA/+}$;*Gsdmd*$^{-/-}$ BMDMs were plated at 10^4 cells per well on a 16-well glass plate overnight. Cells were primed with LPS for 3 hours and pretreated or not with CuET for 15 min before adding 15 μM nigericin (AdipoGen, CA) for 30 min. Cells were washed with PBS and fixed with 4% paraformaldehyde buffer for 10 min at room temperature. For immunostaining, WT and *Nlrp3*$^{CA/+}$;*Gsdmd*$^{-/-}$ BMDMs were permeabilized with 0.2% Triton X-100 in PBS for 20 min; blocked with 0.2% Triton X-100, 1% bovine serum albumin, and CD61 antibody (1:1000; Alexa Fluor 647; BD, NJ) in PBS for 30 min; and were incubated with ASC antibody (1:1000; clone 2EI-7; EMD Millipore, MA) overnight at 4°C in blocking buffer, followed by incubation with secondary antibody (Alexa Fluor 594; Life Technologies) for 30 min. Cells were counterstained with Fluoro-gel II containing 4′,6-diamidino-2-phenylindole (Fluoro-Gel, Fisher Scientific Intl. Inc., PA). Asc-citrine photographs were taken using ZEISS microscopy (Carl Zeiss Industrial Metrology, MN). ASC immunostaining images were taken using a Leica inverted microscope with a TCS SPE II confocal module and processed using LAS X software (Leica Microsystems Inc., IL). Quantification of ASC specks was carried out using ImageJ.

Statistical analysis

Statistical analysis was performed using the Student's *t* test, one-way analysis of variance (ANOVA) with Tukey's multiple comparisons test, or two-way ANOVA with Tukey's multiple comparisons test, Dunnett's multiple comparisons test, or Sidak's multiple comparisons test as well as the log rank (Mantel-Cox) test for comparison of survival curves using the GraphPad Prism 8.0 Software. Values are expressed as means ± SEM or means ± SD, as indicated. $^*P < 0.05$ was considered statistically significant.

SUPPLEMENTARY MATERIALS

www.science.org/doi/10.1126/sciimmunol.abj3859
Figs. S1 to S11
Table S1

View/request a protocol for this paper from *Bio-protocol*.

REFERENCES AND NOTES

1. K. Schroder, J. Tschopp, The inflammasomes. *Cell* **140**, 821–832 (2010).
2. H. Guo, J. B. Callaway, J. P. Ting, Inflammasomes: Mechanism of action, role in disease, and therapeutics. *Nat. Med.* **21**, 677–687 (2015).
3. P. Broz, V. M. Dixit, Inflammasomes: Mechanism of assembly, regulation and signalling. *Nat. Rev. Immunol.* **16**, 407–420 (2016).
4. J. Shi, Y. Zhao, K. Wang, X. Shi, Y. Wang, H. Huang, Y. Zhuang, T. Cai, F. Wang, F. Shao, Cleavage of GSDMD by inflammatory caspases determines pyroptotic cell death. *Nature* **526**, 660–665 (2015).
5. J. Ding, K. Wang, W. Liu, Y. She, Q. Sun, J. Shi, H. Sun, D.-C. Wang, F. Shao, Pore-forming activity and structural autoinhibition of the gasdermin family. *Nature* **535**, 111–116 (2016).
6. C. L. Evavold, J. Ruan, Y. Tan, S. Xia, H. Wu, J. C. Kagan, The pore-forming protein gasdermin D regulates interleukin-1 secretion from living macrophages. *Immunity* **48**, 35–44.e6 (2018).
7. W.-t. He, H. Wan, L. Hu, P. Chen, X. Wang, Z. Huang, Z.-H. Yang, C.-Q. Zhong, J. Han, Gasdermin D is an executor of pyroptosis and required for interleukin-1β secretion. *Cell Res.* **25**, 1285–1298 (2015).
8. X. Liu, Z. Zhang, J. Ruan, Y. Pan, V. G. Magupalli, H. Wu, J. Lieberman, Inflammasome-activated gasdermin D causes pyroptosis by forming membrane pores. *Nature* **535**, 153–158 (2016).
9. S. M. Man, R. Karki, T.-D. Kanneganti, Molecular mechanisms and functions of pyroptosis, inflammatory caspases and inflammasomes in infectious diseases. *Immunol. Rev.* **277**, 61–75 (2017).
10. J. Shi, W. Gao, F. Shao, Pyroptosis: Gasdermin-mediated programmed necrotic cell death. *Trends Biochem. Sci.* **42**, 245–254 (2017).

11. J. C. Mira, L. F. Gentile, B. J. Mathias, P. A. Efron, S. C. Brakenridge, A. M. Mohr, F. A. Moore, L. L. Moldawer, Sepsis pathophysiology, chronic critical illness, and persistent inflammation-immunosuppression and catabolism syndrome. *Crit. Care Med.* **45**, 253–262 (2017).
12. H. M. Hoffman, S. D. Brydges, Genetic and molecular basis of inflammasome-mediated disease. *J. Biol. Chem.* **286**, 10889–10896 (2011).
13. A. A. de Jesus, S. W. Canna, Y. Liu, R. Goldbach-Mansky, Molecular mechanisms in genetically defined autoinflammatory diseases: Disorders of amplified danger signaling. *Annu. Rev. Immunol.* **33**, 823–874 (2015).
14. N. Kayagaki, I. B. Stowe, B. L. Lee, K. O'Rourke, K. Anderson, S. Warming, T. Cuellar, B. Haley, M. Roose-Girma, Q. T. Phung, P. S. Liu, J. R. Lill, H. Li, J. Wu, S. Kummerfeld, J. Zhang, W. P. Lee, S. J. Snipas, G. S. Salvesen, L. X. Morris, L. Fitzgerald, Y. Zhang, E. M. Bertram, C. C. Goodnow, V. M. Dixit, Caspase-11 cleaves gasdermin D for non-canonical inflammasome signalling. *Nature* **526**, 666–671 (2015).
15. H. Kambara, F. Liu, X. Zhang, P. Liu, B. Bajrami, Y. Teng, L. Zhao, S. Zhou, H. Yu, W. Zhou, L. E. Silberstein, T. Cheng, M. Han, Y. Xu, H. R. Luo, Gasdermin D exerts anti-inflammatory effects by promoting neutrophil death. *Cell Rep.* **22**, 2924–2936 (2018).
16. M. Karmakar, M. Minns, E. N. Greenberg, J. Diaz-Aponte, K. Pestonjamasp, J. L. Johnson, J. K. Rathkey, D. W. Abbott, K. Wang, F. Shao, S. D. Catz, G. R. Dubyak, E. Pearlman, N-GSDMD trafficking to neutrophil organelles facilitates IL-1β release independently of plasma membrane pores and pyroptosis. *Nat. Commun.* **11**, 2212 (2020).
17. K. W. Chen, M. Monteleone, D. Boucher, G. Sollberger, D. Ramnath, N. D. Condon, J. B. von Pein, P. Broz, M. J. Sweet, K. Schroder, Noncanonical inflammasome signaling elicits gasdermin D-dependent neutrophil extracellular traps. *Sci. Immunol.* **3**, eaar6676 (2018).
18. S. S. Burgener, N. G. F. Leborgne, S. J. Snipas, G. S. Salvesen, P. I. Bird, C. Benarafa, Cathepsin G inhibition by Serpinb1 and Serpinb6 prevents programmed necrosis in neutrophils and monocytes and reduces GSDMD-driven inflammation. *Cell Rep.* **27**, 3646–3656.e5 (2019).
19. K. W. Chen, B. Demarco, R. Heilig, K. Shkarina, A. Boettcher, C. J. Farady, P. Pelczar, P. Broz, Extrinsic and intrinsic apoptosis activate pannexin-1 to drive NLRP3 inflammasome assembly. *EMBO J.* **38**, e101638 (2019).
20. J. Sarhan, B. C. Liu, H. I. Muendlein, P. Li, R. Nilson, A. Y. Tang, A. Rongvaux, S. C. Bunnell, F. Shao, D. R. Green, A. Poltorak, Caspase-8 induces cleavage of gasdermin D to elicit pyroptosis during *Yersinia* infection. *Proc. Natl. Acad. Sci. U.S.A.* **115**, E10888–E10897 (2018).
21. P. Orning, D. Weng, K. Starheim, D. Ratner, Z. Best, B. Lee, A. Brooks, S. Xia, H. Wu, M. A. Kelliher, S. B. Berger, P. J. Gough, J. Bertin, M. M. Proulx, J. D. Goguen, N. Kayagaki, K. A. Fitzgerald, E. Lien, Pathogen blockade of TAK1 triggers caspase-8–dependent cleavage of gasdermin D and cell death. *Science* **362**, 1064–1069 (2018).
22. C. Rogers, T. Fernandes-Alnemri, L. Mayes, D. Alnemri, G. Cingolani, E. S. Alnemri, Cleavage of DFNA5 by caspase-3 during apoptosis mediates progression to secondary necrotic/pyroptotic cell death. *Nat. Commun.* **8**, 14128 (2017).
23. Z. Zhang, Y. Zhang, S. Xia, Q. Kong, S. Li, X. Liu, C. Junqueira, K. F. Meza-Sosa, T. M. Y. Mok, J. Ansara, S. Sengupta, Y. Yao, H. Wu, J. Lieberman, Gasdermin E suppresses tumour growth by activating anti-tumour immunity. *Nature* **579**, 415–420 (2020).
24. C. Rogers, D. A. Erkes, A. Nardone, A. E. Aplin, T. Fernandes-Alnemri, E. S. Alnemri, Gasdermin pores permeabilize mitochondria to augment caspase-3 activation during apoptosis and inflammasome activation. *Nat. Commun.* **10**, 1689 (2019).
25. Y. Wang, W. Gao, X. Shi, J. Ding, W. Liu, H. He, K. Wang, F. Shao, Chemotherapy drugs induce pyroptosis through caspase-3 cleavage of a gasdermin. *Nature* **547**, 99–103 (2017).
26. J. Yu, S. Li, J. Qi, Z. Chen, Y. Wu, J. Guo, K. Wang, X. Sun, J. Zheng, Cleavage of GSDME by caspase-3 determines lobaplatin-induced pyroptosis in colon cancer cells. *Cell Death Dis.* **10**, 193 (2019).
27. K. Tsuchiya, S. Nakajima, S. Hosojima, D. Thi Nguyen, T. Hattori, T. Manh Le, O. Hori, M. R. Mahib, Y. Yamaguchi, M. Miura, T. Kinoshita, H. Kushiyama, M. Sakurai, T. Shiroishi, T. Suda, Caspase-1 initiates apoptosis in the absence of gasdermin D. *Nat. Commun.* **10**, 2091 (2019).
28. E. Aizawa, T. Karasawa, S. Watanabe, T. Komada, H. Kimura, R. Kamata, H. Ito, E. Hishida, N. Yamada, T. Kasahara, Y. Mori, M. Takahashi, GSDME-dependent incomplete pyroptosis permits selective IL-1α release under caspase-1 inhibition. *iScience* **23**, 101070 (2020).
29. Y. Liu, Y. Fang, X. Chen, Z. Wang, X. Liang, T. Zhang, M. Liu, N. Zhou, J. Lv, K. Tang, J. Xie, Y. Gao, F. Cheng, Y. Zhou, Z. Zhang, Y. Hu, X. Zhang, Q. Gao, Y. Zhang, B. Huang, Gasdermin E-mediated target cell pyroptosis by CAR T cells triggers cytokine release syndrome. *Sci. Immunol.* **5**, eaax7969 (2020).
30. R. Tixeira, B. Shi, M. A. F. Parkes, A. L. Hodge, S. Caruso, M. D. Hulett, A. A. Baxter, T. K. Phan, I. K. H. Poon, Gasdermin E does not limit apoptotic cell disassembly by promoting early onset of secondary necrosis in Jurkat T cells and THP-1 monocytes. *Front. Immunol.* **9**, 2842 (2018).
31. B. L. Lee, K. M. Mirrashidi, I. B. Stowe, S. K. Kummerfeld, C. Watanabe, B. Haley, T. L. Cuellar, M. Reichelt, N. Kayagaki, ASC- and caspase-8-dependent apoptotic pathway diverges from the NLRC4 inflammasome in macrophages. *Sci. Rep.* **8**, 3788 (2018).
32. R. Heilig, M. Dilucca, D. Boucher, K. W. Chen, D. Hancz, B. Demarco, K. Shkarina, P. Broz, Caspase-1 cleaves Bid to release mitochondrial SMAC and drive secondary necrosis in the absence of GSDMD. *Life Sci. Alliance* **3**, e202000735 (2020).
33. J. E. Vince, D. De Nardo, W. Gao, A. J. Vince, C. Hall, K. McArthur, D. Simpson, S. Vijayaraj, L. M. Lindqvist, P. Bouillet, M. A. Rizzacasa, S. M. Man, J. Silke, S. L. Masters, G. Lessene, D. C. S. Huang, D. H. D. Gray, B. T. Kile, F. Shao, K. E. Lawlor, The mitochondrial apoptotic effectors BAX/BAK activate caspase-3 and -7 to trigger NLRP3 inflammasome and caspase-8 driven IL-1β activation. *Cell Rep.* **25**, 2339–2353.e4 (2018).
34. H. H. Shen, Y. X. Yang, X. Meng, X. Y. Luo, X. M. Li, Z. W. Shuai, D. Q. Ye, H. F. Pan, NLRP3: A promising therapeutic target for autoimmune diseases. *Autoimmun. Rev.* **17**, 694–702 (2018).
35. L. P. Zambetti, A. Mortellaro, NLRPs, microbiota, and gut homeostasis: Unravelling the connection. *J. Pathol.* **233**, 321–330 (2014).
36. Y. Zhen, H. Zhang, NLRP3 inflammasome and inflammatory bowel disease. *Front. Immunol.* **10**, 276 (2019).
37. L. Spel, F. Martinon, Inflammasomes contributing to inflammation in arthritis. *Immunol. Rev.* **294**, 48–62 (2020).
38. E. Jäger, S. Murthy, C. Schmidt, M. Hahn, S. Strobel, A. Peters, C. Stäubert, P. Sungur, T. Venus, M. Geisler, V. Radusheva, S. Raps, K. Rothe, R. Scholz, S. Jung, S. Wagner, M. Pierer, O. Seifert, W. Chang, I. Estrela-Lopis, N. Raulien, K. Krohn, N. Sträter, S. Hoeppener, T. Schöneberg, M. Rossol, U. Wagner, Calcium-sensing receptor-mediated NLRP3 inflammasome response to calciprotein particles drives inflammation in rheumatoid arthritis. *Nat. Commun.* **11**, 4243 (2020).
39. Y. Alippe, G. Mbalaviele, Omnipresence of inflammasome activities in inflammatory bone diseases. *Semin. Immunopathol.* **41**, 607–618 (2019).
40. T. Zhuang, J. Liu, X. Chen, L. Zhang, J. Pi, H. Sun, L. Li, R. Bauer, H. Wang, Z. Yu, Q. Zhang, B. Tomlinson, P. Chan, X. Zheng, E. Morrisey, Z. Liu, M. Reilly, Y. Zhang, Endothelial Foxp1 suppresses atherosclerosis via modulation of Nlrp3 inflammasome activation. *Circ. Res.* **125**, 590–605 (2019).
41. A. Grebe, F. Hoss, E. Latz, NLRP3 inflammasome and the IL-1 pathway in atherosclerosis. *Circ. Res.* **122**, 1722–1740 (2018).
42. S. C. Eisenbarth, R. A. Flavell, Innate instruction of adaptive immunity revisited: The inflammasome. *EMBO Mol. Med.* **1**, 92–98 (2009).
43. F. Renaudin, L. Orliaguet, F. Castelli, F. Fenaille, A. Prignon, F. Alzaid, C. Combes, A. Delvaux, Y. Adimy, M. Cohen-Solal, P. Richette, T. Bardin, J. P. Riveline, N. Venteclef, F. Lioté, L. Campillo-Gimenez, H. K. Ea, Gout and pseudo-gout-related crystals promote GLUT1-mediated glycolysis that governs NLRP3 and interleukin-1β activation on macrophages. *Ann. Rheum. Dis.* **79**, 1506–1514 (2020).
44. N. Dalbeth, H. K. Choi, L. A. B. Joosten, P. P. Khanna, H. Matsuo, F. Perez-Ruiz, L. K. Stamp, Gout. *Nat. Rev. Dis. Primers.* **5**, 69 (2019).
45. F. Martinon, V. Pétrilli, A. Mayor, A. Tardivel, J. Tschopp, Gout-associated uric acid crystals activate the NALP3 inflammasome. *Nature* **440**, 237–241 (2006).
46. S. Ding, S. Xu, Y. Ma, G. Liu, H. Jang, J. Fang, Modulatory mechanisms of the NLRP3 inflammasomes in diabetes. *Biomolecules* **9**, 850 (2019).
47. I. Aksentijevich, M. Nowak, M. Mallah, J. J. Chae, W. T. Watford, S. R. Hofmann, L. Stein, R. Russo, D. Goldsmith, P. Dent, H. F. Rosenberg, F. Austin, E. F. Remmers, J. E. Balow Jr., S. Rosenzweig, H. Komarow, N. G. Shoham, G. Wood, J. Jones, N. Mangra, H. Carrero, B. S. Adams, T. L. Moore, K. Schikler, H. Hoffman, D. J. Lovell, R. Lipnick, K. Barron, J. J. O'Shea, D. L. Kastner, R. Goldbach-Mansky, De novo CIAS1 mutations, cytokine activation, and evidence for genetic heterogeneity in patients with neonatal-onset multisystem inflammatory disease (NOMID): A new member of the expanding family of pyrin-associated autoinflammatory diseases. *Arthritis Rheum.* **46**, 3340–3348 (2002).
48. F. M. Zaki, R. Sridharan, T. S. Pei, S. Ibrahim, T. S. Ping, NOMID: The radiographic and MRI features and review of literature. *J. Radiol. Case Rep.* **6**, 1–8 (2012).
49. S. C. Hill, M. Namde, A. Dwyer, A. Poznanski, S. Canna, R. Goldbach-Mansky, Arthropathy of neonatal onset multisystem inflammatory disease (NOMID/CINCA). *Pediatr. Radiol.* **37**, 145–152 (2007).
50. J. Feldmann, A.-M. Prieur, P. Quartier, P. Berquin, S. Certain, E. Cortis, D. Teillac-Hamel, A. Fischer, G. de Saint Basile, Chronic infantile neurological cutaneous and articular syndrome is caused by mutations in CIAS1, a gene highly expressed in polymorphonuclear cells and chondrocytes. *Am. J. Hum. Genet.* **71**, 198–203 (2002).
51. H. M. Hoffman, J. L. Mueller, D. H. Broide, A. A. Wanderer, R. D. Kolodner, Mutation of a new gene encoding a putative pyrin-like protein causes familial cold autoinflammatory syndrome and Muckle-Wells syndrome. *Nat. Genet.* **29**, 301–305 (2001).
52. S. L. Bonar, S. D. Brydges, J. L. Mueller, M. D. McGeough, C. Pena, D. Chen, S. K. Grimston, C. L. Hickman-Brecks, S. Ravindran, A. McAlinden, D. V. Novack, D. L. Kastner, R. Civitelli, H. M. Hoffman, G. Mbalaviele, Constitutively activated NLRP3 inflammasome causes inflammation and abnormal skeletal development in mice. *PLOS ONE* **7**, e35979 (2012).
53. S. D. Brydges, L. Broderick, M. D. McGeough, C. A. Pena, J. L. Mueller, H. M. Hoffman, Divergence of IL-1, IL-18, and cell death in NLRP3 inflammasomopathies. *J. Clin. Invest.* **123**, 4695–4705 (2013).

54. C. Wang, C. X. Xu, Y. Alippe, C. Qu, J. Xiao, E. Schipani, R. Civitelli, Y. Abu-Amer, G. Mbalaviele, Chronic inflammation triggered by the NLRP3 inflammasome in myeloid cells promotes growth plate dysplasia by mesenchymal cells. *Sci. Rep.* **7**, 4880 (2017).
55. M. D. McGeough, A. Wree, M. E. Inzaugarat, A. Haimovich, C. D. Johnson, C. A. Peña, R. Goldbach-Mansky, L. Broderick, A. E. Feldstein, H. M. Hoffman, TNF regulates transcription of NLRP3 inflammasome components and inflammatory molecules in cryopyrinopathies. *J. Clin. Invest.* **127**, 4488–4497 (2017).
56. J. Xiao, C. Wang, J. C. Yao, Y. Alippe, C. Xu, D. Kress, R. Civitelli, Y. Abu-Amer, T. D. Kanneganti, D. C. Link, G. Mbalaviele, Gasdermin D mediates the pathogenesis of neonatal-onset multisystem inflammatory disease in mice. *PLoS Biol.* **16**, e3000047 (2018).
57. A. Kanneganti, R. K. S. Malireddi, P. H. V. Saavedra, L. Vande Walle, H. Van Gorp, H. Kambara, H. Tillman, P. Vogel, H. R. Luo, R. J. Xavier, H. Chi, M. Lamkanfi, GSDMD is critical for autoinflammatory pathology in a mouse model of Familial Mediterranean Fever. *J. Exp. Med.* **215**, 1519–1529 (2018).
58. S. Li, Y. Wu, D. Yang, C. Wu, C. Ma, X. Liu, P. N. Moynagh, B. Wang, G. Hu, S. Yang, Gasdermin D in peripheral myeloid cells drives neuroinflammation in experimental autoimmune encephalomyelitis. *J. Exp. Med.* **216**, 2562–2581 (2019).
59. N. Ter Haar, H. Lachmann, S. Özen, P. Woo, Y. Uziel, C. Modesto, I. Koné-Paut, L. Cantarini, A. Insalaco, B. Neven, M. Hofer, D. Rigante, S. Al-Mayouf, I. Touitou, R. Gallizzi, E. Papadopoulou-Alataki, S. Martino, J. Kuemmerle-Deschner, L. Obici, N. Iagaru, A. Simon, S. Nielsen, A. Martini, N. Ruperto, M. Gattorno, J. Frenkel; Paediatric Rheumatology International Trials Organisation (PRINTO) and the Eurofever/Eurotraps Projects, Treatment of autoinflammatory diseases: Results from the Eurofever Registry and a literature review. *Ann. Rheum. Dis.* **72**, 678–685 (2013).
60. J. Anton, I. Calvo, J. Fernández-Martin, M. L. Gamir, R. Merino, S. Jimenez-Treviño, B. Sevilla, F. Cabades, R. Bou, J. I. Arostegui, Efficacy and safety of canakinumab in cryopyrin-associated periodic syndromes: Results from a Spanish cohort. *Clin. Exp. Rheumatol.* **33**, S67–S71 (2015).
61. C. H. Sibley, N. Plass, J. Snow, E. A. Wiggs, C. C. Brewer, K. A. King, C. Zalewski, H. J. Kim, R. Bishop, S. Hill, S. M. Paul, P. Kicker, Z. Phillips, J. G. Dolan, B. Widemann, N. Jayaprakash, F. Pucino, D. L. Stone, D. Chapelle, C. Snyder, J. A. Butman, R. Wesley, R. Goldbach-Mansky, Sustained response and prevention of damage progression in patients with neonatal-onset multisystem inflammatory disease treated with anakinra: A cohort study to determine three- and five-year outcomes. *Arthritis Rheum.* **64**, 2375–2386 (2012).
62. B. Neven, I. Marvillet, C. Terrada, A. Ferster, N. Boddaert, V. Couloignier, G. Pinto, A. Pagnier, C. Bodemer, B. Bodaghi, M. Tardieu, A. M. Prieur, P. Quartier, Long-term efficacy of the interleukin-1 receptor antagonist anakinra in ten patients with neonatal-onset multisystem inflammatory disease/chronic infantile neurologic, cutaneous, articular syndrome. *Arthritis Rheum.* **62**, 258–267 (2010).
63. D. Rigante, A. Leone, R. Marrocco, M. E. Laino, A. Stabile, Long-term response after 6-year treatment with anakinra and onset of focal bone erosion in neonatal-onset multisystem inflammatory disease (NOMID/CINCA). *Rheumatol. Int.* **31**, 1661–1664 (2011).
64. F. Humphries, L. Shmuel-Galia, N. Ketelut-Carneiro, S. Li, B. Wang, V. V. Nemmara, R. Wilson, Z. Jiang, F. Khalighinejad, K. Muneeruddin, S. A. Shaffer, R. Dutta, C. Ionete, S. Pesiridis, S. Yang, P. R. Thompson, K. A. Fitzgerald, Succination inactivates gasdermin D and blocks pyroptosis. *Science* **369**, 1633–1637 (2020).
65. J. J. Hu, X. Liu, S. Xia, Z. Zhang, Y. Zhang, J. Zhao, J. Ruan, X. Luo, X. Lou, Y. Bai, J. Wang, L. R. Hollingsworth, V. G. Magupalli, L. Zhao, H. R. Luo, J. Kim, J. Lieberman, H. Wu, FDA-approved disulfiram inhibits pyroptosis by blocking gasdermin D pore formation. *Nat. Immunol.* **21**, 736–745 (2020).
66. W. Deng, Z. Yang, H. Yue, Y. Ou, W. Hu, P. Sun, Disulfiram suppresses NLRP3 inflammasome activation to treat peritoneal and gouty inflammation. *Free Radic. Biol. Med.* **152**, 8–17 (2020).
67. S. D. Brydges, J. L. Mueller, M. D. McGeough, C. A. Pena, A. Misaghi, C. Gandhi, C. D. Putnam, D. L. Boyle, G. S. Firestein, A. A. Horner, P. Soroosh, W. T. Watford, J. J. O'Shea, D. L. Kastner, H. M. Hoffman, Inflammasome-mediated disease animal models reveal roles for innate but not adaptive immunity. *Immunity* **30**, 875–887 (2009).
68. J. N. Snouwaert, M. Nguyen, P. W. Repenning, R. Dye, E. W. Livingston, M. Kovarova, S. S. Moy, B. E. Brigman, T. A. Bateman, J. P. Ting, B. H. Koller, An NLRP3 mutation causes arthropathy and osteoporosis in humanized mice. *Cell Rep.* **17**, 3077–3088 (2016).
69. S. E. Garnish, Y. Meng, A. Koide, J. J. Sandow, E. Denbaum, A. V. Jacobsen, W. Yeung, A. L. Samson, C. R. Horne, C. Fitzgibbon, S. N. Young, P. P. C. Smith, A. I. Webb, E. J. Petrie, J. M. Hildebrand, N. Kannan, P. E. Czabotar, S. Koide, J. M. Murphy, Conformational interconversion of MLKL and disengagement from RIPK3 precede cell death by necroptosis. *Nat. Commun.* **12**, 2211 (2021).
70. L. Sun, H. Wang, Z. Wang, S. He, S. Chen, D. Liao, L. Wang, J. Yan, W. Liu, X. Lei, X. Wang, Mixed lineage kinase domain-like protein mediates necrosis signaling downstream of RIP3 kinase. *Cell* **148**, 213–227 (2012).
71. C. Y. Taabazuing, M. C. Okondo, D. A. Bachovchin, Pyroptosis and apoptosis pathways engage in bidirectional crosstalk in monocytes and macrophages. *Cell Chem. Biol.* **24**, 507–514.e4 (2017).
72. A. Baroja-Mazo, F. Martín-Sánchez, A. I. Gomez, C. M. Martínez, J. Amores-Iniesta, V. Compan, M. Barberà-Cremades, J. Yagüe, E. Ruiz-Ortiz, J. Antón, S. Buján, I. Couillin, D. Brough, J. I. Arostegui, P. Pelegrín, The NLRP3 inflammasome is released as a particulate danger signal that amplifies the inflammatory response. *Nat. Immunol.* **15**, 738–748 (2014).
73. B. S. Franklin, L. Bossaller, D. De Nardo, J. M. Ratter, A. Stutz, G. Engels, C. Brenker, M. Nordhoff, S. R. Mirandola, A. Al-Amoudi, M. S. Mangan, S. Zimmer, B. G. Monks, M. Fricke, R. E. Schmidt, T. Espevik, B. Jones, A. G. Jarnicki, P. M. Hansbro, P. Busto, A. Marshak-Rothstein, S. Hornemann, A. Aguzzi, W. Kastenmüller, E. Latz, The adaptor ASC has extracellular and "prionoid" activities that propagate inflammation. *Nat. Immunol.* **15**, 727–737 (2014).
74. P. Sagoo, Z. Garcia, B. Breart, F. Lemaître, D. Michonneau, M. L. Albert, Y. Levy, P. Bousso, In vivo imaging of inflammasome activation reveals a subcapsular macrophage burst response that mobilizes innate and adaptive immunity. *Nat. Med.* **22**, 64–71 (2016).
75. S. R. Mihaly, J. Ninomiya-Tsuji, S. Morioka, TAK1 control of cell death. *Cell Death Differ.* **21**, 1667–1676 (2014).
76. H. Legros, F. Janin, N. Dourmap, J.-J. Bonnet, J. Costentin, Semi-chronic increase in striatal level of 3,4-dihydroxyphenylacetaldehyde does not result in alteration of nigrostriatal dopaminergic neurones. *J. Neurosci. Res.* **75**, 429–435 (2004).
77. C. Qu, S. L. Bonar, C. L. Hickman-Brecks, S. Abu-Amer, M. D. McGeough, C. A. Peña, L. Broderick, C. Yang, S. K. Grimston, J. Kading, Y. Abu-Amer, D. V. Novack, H. M. Hoffman, R. Civitelli, G. Mbalaviele, NLRP3 mediates osteolysis through inflammation-dependent and -independent mechanisms. *FASEB J.* **29**, 1269–1279 (2015).
78. A. Volchuk, A. Ye, L. Chi, B. E. Steinberg, N. M. Goldenberg, Indirect regulation of HMGB1 release by gasdermin D. *Nat. Commun.* **11**, 4561 (2020).
79. N. Kayagaki, O. S. Kornfeld, B. L. Lee, I. B. Stowe, K. O'Rourke, Q. Li, W. Sandoval, D. Yan, J. Kang, M. Xu, J. Zhang, W. P. Lee, B. S. McKenzie, G. Ulas, J. Payandeh, M. Roose-Girma, Z. Modrusan, R. Reja, M. Sagolla, J. D. Webster, V. Cho, T. D. Andrews, L. X. Morris, L. A. Miosge, C. C. Goodnow, E. M. Bertram, V. M. Dixit, NINJ1 mediates plasma membrane rupture during lytic cell death. *Nature* **591**, 131–136 (2021).
80. J. Tschopp, K. Schroder, NLRP3 inflammasome activation: The convergence of multiple signalling pathways on ROS production? *Nat. Rev. Immunol.* **10**, 210–215 (2010).
81. C. Wang, S. Hockerman, E. J. Jacobsen, Y. Alippe, S. R. Selness, H. R. Hope, J. L. Hirsch, S. J. Mnich, M. J. Saabye, W. F. Hood, S. L. Bonar, Y. Abu-Amer, A. Haimovich, H. M. Hoffman, J. B. Monahan, G. Mbalaviele, Selective inhibition of the p38α MAPK-MK2 axis inhibits inflammatory cues including inflammasome priming signals. *J. Exp. Med.* **215**, 1315–1325 (2018).
82. S. Takeshita, K. Kaji, A. Kudo, Identification and characterization of the new osteoclast progenitor with macrophage phenotypes being able to differentiate into mature osteoclasts. *J. Bone Miner. Res.* **15**, 1477–1488 (2000).

Acknowledgments: We want to thank D. J. Veis for critical reading of this manuscript. **Funding:** This work was supported by NIH/NIAMS AR068972 and AR076758 grants to G.M. Y.A.-A. was supported by NIH grants AR049192 and AR072623 and by a grant no. 85160 from the Shriners Hospital for Children. **Author contributions:** Conceptualization: C.W. and G.M. Methodology: C.W., T.Y., J.X., C.X., Y.A., K.S., and G.M. Writing (original draft): C.W. and G.M. Writing (review and editing): C.W., T.-D.K., J.B.M., Y.A.-A., J.L., and G.M. **Competing interests:** G.M. is consultant for Aclaris Therapeutics Inc. C.X. and J.B.M. are employees of Aclaris Therapeutics Inc. J.L. is cofounder and SAB member of Ventus Therapeutics and has filed a patent application for the use of disulfiram for inhibiting pyroptosis and inflammation. All other authors declare that they have no competing financial interests. **Data and materials availability:** All data needed to evaluate the conclusions in the paper are present in the paper or the Supplementary Materials.

Submitted 9 May 2021
Accepted 9 September 2021
Published 22 October 2021
10.1126/sciimmunol.abj3859

Citation: C. Wang, T. Yang, J. Xiao, C. Xu, Y. Alippe, K. Sun, T.-D. Kanneganti, J. B. Monahan, Y. Abu-Amer, J. Lieberman, G. Mbalaviele, NLRP3 inflammasome activation triggers gasdermin D–independent inflammation. *Sci. Immunol.* **6**, eabj3859 (2021).

Science Immunology

NLRP3 inflammasome activation triggers gasdermin D–independent inflammation

Chun WangTong YangJianqiu XiaoCanxin XuYael AlippeKai SunThirumala-Devi KanneganTiJoseph B. MonahanYousef Abu-AmerJudy LiebermanGabriel Mbalaviele

Sci. Immunol., 6 (64), eabj3859. • DOI: 10.1126/sciimmunol.abj3859

An unexpected path for inflammasome-mediated inflammation

Many inflammatory disorders are linked to an overactive NLRP3 inflammasome due to increased cell death and production of inflammatory cytokines. In some cases, targeting the pyroptosis (an inflammatory form of cell death) pore-forming unit gasdermin D (GSDMD) alleviates these disorders, but the direct role of GSDMD during sustained NLRP3 inflammasome activation is unclear. Using various knockout mouse models, Wang *et al*. determined that constitutive NLRP3 activation was able to still induce inflammation in the absence of GSDMD seemingly through GSDME-mediated pyroptosis. NLRP3 overactivation–associated pathologies could be inhibited by pharmacologically targeting both GSDMD and GSDME activation with CuET. Thus, this work presents a potential treatment for inflammatory disorders caused by sustained NLRP3 inflammasome activation.

Science Immunology (ISSN) is published by the American Association for the Advancement of Science. 1200 New York Avenue NW, Washington, DC 20005. The title *Science Immunology* is a registered trademark of AAAS.